

## Fossil catfishes of the families Doradidae and Pimelodidae (Teleostei: Siluriformes) from the Miocene Urumaco Formation of Venezuela

MARK H. SABAJ PÉREZ

*Department of Ichthyology, The Academy of Natural Sciences, 1900 Benjamin Franklin Parkway, Philadelphia, PA 19103-1195, USA*

ORANGEL A. AGUILERA S.

*Universidad Nacional Experimental Francisco de Miranda, Centro de Investigaciones en Ciencias Básicas, Complejo Docente Los Perozos, Carretera Variante Sur, Coro, 4101, Falcón, VENEZUELA*

JOHN G. LUNDBERG

*Department of Ichthyology, The Academy of Natural Sciences, 1900 Benjamin Franklin Parkway, Philadelphia, PA 19103-1195, USA*

**ABSTRACT.**—Four taxa are added to the fossil history of catfishes based on new identifications and descriptions of material from the Miocene Urumaco Formation in northwestern Venezuela. Three of the fossil catfishes belong to the family Doradidae (thorny catfishes); one, *Doras dioneae*, represents a new species, the first fossil doradid to be formally named, and the other two, *Doraops* cf. *zuloagai* and *Rhinodoras* cf. *thomersoni*, are referred to modern taxa endemic to the Maracaibo basin. The fourth fossil catfish belongs to the family Pimelodidae (long-whiskered catfishes) and is assigned to *Platysilurus*, a modern genus that occurs in the Maracaibo, Orinoco, Amazon, and large rivers of the Guianas. These fossil taxa inhabited the paleo-Amazon-Orinoco, a large ancient river system that drained the South American continent northward prior to the uplift of the Eastern Andes and Coastal Cordilleras and concomitant isolation of the Maracaibo basin in the Late Miocene (ca. 8 Ma).

Species novum: *Doras dioneae* Sabaj Pérez, Aguilera and Lundberg

---

### INTRODUCTION

The Doradidae (thorny catfishes) are a monophyletic family endemic to South America (Sabaj and Ferraris, 2003). Most thorny catfishes are restricted to freshwaters and typically inhabit large lowland river systems; however, two species approach or may enter brackish waters either near the mouths of large rivers (*Lithodoras dorsalis*) or along the shores of Lake Maracaibo (*Doraops zuloagai*). The living doradid fauna includes 30 genera with a total of about 80 species distributed in the Amazon-Tocantins (ca. 59 species), Orinoco (24), coastal drainages of the Guianas (20), Paraná-Paraguay (7), coastal drainages of eastern Brazil (6), Maracaibo (2), and Magdalena (1). The fossil history of thorny catfishes is too scarce and fragmentary to provide major insights into the early evolution of the group. Lundberg (1997) reported indeterminate doradid fossils among the La Venta fauna of the Middle Miocene Honda Group dated 11.6 to 13.5 or 13.8 Ma (Flynn et al., 1997) and located in the present-day Magdalena River valley, Colombia. Other records of indeterminate fossil doradids

are from the Miocene Ituzaingó Formation, Paraná, Argentina (Cione, 1978; 1986; Arratia and Cione, 1996) and Miocene deposits in the Acre River region, Brazil and Peru (Arratia and Cione, 1996; Lundberg, 1998:61). Aguilera (2004) figured and briefly described from the Miocene Urumaco formation in Venezuela fossils tentatively identified as *Oxydoras* sp. (neurocranium and nuchal shield), cf. *Doras* sp. (pectoral girdle and spine) and cf. *Rhinodoras* sp. (pectoral girdle and spine). These fossils are reidentified and described herein as *Rhinodoras* cf. *thomersoni*, *Doras dioneae*, n. sp. and *Doraops* cf. *zuloagai*, respectively.

The Pimelodidae (long-whiskered catfishes) are endemic to South and Central America and comprise about 32 living genera and 86 species. Fossil pimelodids are previously known in the South American record by two goliath catfishes: *Brachyplatystoma* cf. *vallantii* (Lundberg, 1997) and *B. progmagdalena* (Lundberg, 2005), both from the Middle Miocene Honda Group in Colombia. Additionally, there are two fossil species of redbtail catfishes: *Phractocephalus nassi* (Lundberg and Aguilera, 2003) from the Late Miocene Urumaco Formation in Venezuela, and an

undescribed species under study by Aguilera, Bocquentin and Lundberg from the Late Miocene-Pliocene Solimões Formation in Brazil. Other records of indeterminate fossil pimelodids are from the Miocene deposits in the Acre River region, Brazil (Lundberg, unpubl. data).

The findings of additional fossil species of Doradidae and Pimelodidae in the Late Miocene Urumaco Formation, northwestern Venezuela, support the hypothesis of Lundberg (1998), who suggested that the late middle Miocene neotropical fish fauna was essentially modern across a wide taxonomic and ecological range. Furthermore, fossil fish from Urumaco are of significance in providing information about the past history of the fluvial systems on the South American continent.

#### MATERIALS AND METHODS

Fossils were collected during several expeditions to the Urumaco Formation between 1994 and 2005 by teams from the UNEFM. The sample area (Fig. 1) includes the following named localities: El Mamón, Tío Gregorio, Corralito and El Hatillo, all north of the town of Urumaco, Falcón State, northwestern Venezuela. A late Miocene age for the Urumaco Formation is indicated by foraminiferans, and the mammals suggest a South American land mammal age between Chasicoan and Huayquerian (Díaz de Gamero and Linares, 1989), or approximately 9 Ma (Marshall and Sempere, 1993).

Geological units from which the specimens were obtained are the middle and upper members of the Urumaco Formation (summarized in Ministerio de Energía y Minas, 1997). The middle member of the Urumaco Formation consists of gray and brown claystone and sand. The gray claystone is microfossiliferous, and the brown claystone contains vertebrate remains such as reptiles, mammals, marine and freshwater fish, in addition to coprolites and wood (Aguilera, 2004; Díaz de Gamero and Linares, 1989). The limestone changes from conchiferous sandstones to consolidated coquina limestone. The paleoenvironments are interpreted as inner sub-littoral and coastal lagoon environments with riverine and estuarine influence (Aguilera, 2004; Díaz de Gamero, 1996).

The upper member of the Urumaco Formation also comprises gray to brown, often limey claystone with thin intercalated and locally conchiferous sandstones. The uppermost layer is referred to as the “capa de tortugas” because of its abundant remains of the turtle *Bairdemys*. Several localities and levels have concentrations of vertebrate fossils. The vertebrate fauna includes marine, estuarine and freshwater fishes, terrestrial, freshwater and marine turtles and crocodylians, and terrestrial and aquatic/semiaquatic mammals (Aguilera, 2004; Sánchez-Villagra et al., 2003;

Sánchez-Villagra and Aguilera, 2006). Based on Hambalek et al. (1994) the palaeoenvironments in the upper member included tropical near-shore marine to low coastal savannas submitted to tidal wave and freshwater flow, surrounded by mangrove vegetation.

The fossils treated here are three-dimensional articulated crania and disarticulated post-cranial, usually abraded broken bones obtained individually from surface exposures in the field. Matrix materials surrounding Urumaco specimens vary from fine, loose sand that was removed with brushes, to iron-stained claystone requiring softening with water and manual cleaning with fine tipped dental tools.

Fossils were identified by direct comparison to each other and to dry skeletons and alcohol preserved specimens of modern fishes (Appendices 1 and 2). Diagnoses and descriptions are aggregate, based on the sum of features exhibited by the fossils considered to be conspecific by comparison to modern taxa. Measurements were taken with digital calipers to the nearest 0.1 mm. Measurement data of fossils emphasize overall specimen size and, as preservation allows, landmark-based linear dimensions for proportional (shape) comparisons with extant species. Measurements of postcleithral process in doradids include (Fig. 2E): dorsal length = distance from anterior point or corner (landmark 1) defined by intersection of curved posterior margin of smooth anterolateral face of cleithrum (underlying posterior margin of fleshy opercle flap in life) and raised dorsal margin of postcleithral process (i.e., point where dorsal margin first appears distinctly elevated, via shelf, from dorsal limb of cleithrum) to posteriormost point (2) along dorsal margin of process (= dorsal posterior corner in *Doras*); ventral length = distance from anterior point (indentation, 3) marking juncture of ventral margin of shoulder buldge (part of cleithrum receiving dorsal process of pectoral spine) and ventral margin of postcleithral process to posteriormost point (4) along ventral margin of process (= ventral posterior corner in *Doras*); oblique length = distance from anteriormost point (1) along raised dorsal margin of process (as described for dorsal length) to posteriormost tip (4) of process (= ventral posterior corner in *Doras*, measurement same as postcleithral process length in Sabaj, 2005:640); depth = greatest depth orthogonal to straight line formed by long axis of process. Measurements of nuchal shield in doradids include: minimum width = minimum transverse distance between concave lateral margins of middle nuchal plate; length = middorsal distance from suture between supraoccipital and anterior nuchal plate to posterior rim of middle nuchal plate (anterior to origin of dorsal-locking spine).

Osteological and other abbreviations are listed in Appendix 3. Major bony elements are abbreviated with three capital letters; parts of bones, structures involving more than



Fig. 1. Location of fossil sampling sites discussed in text. El Mamón, Tío Gregorio, Corralito, El Hatillo and El Picache, are all north of town of Urumaco, Falcón State, northwestern Venezuela.

one bone, or non-bony features are indicated in lower-case letters. Institutional abbreviations as in Leviton et al. (1985) with the addition of UNEFM for Universidad Nacional Experimental Francisco de Miranda, Coro, Falcón State, Venezuela.

Order Siluriformes *sensu* Berg, 1940  
 Family Doradidae *sensu* Sabaj and Ferraris, 2003  
 Genus *Doras* Lacépède, 1803

†*Doras dioneae* Sabaj Pérez, Aguilera and Lundberg, n. sp.  
 Figs. 2, 4

cf. *Doras* sp. in Aguilera 2004:62 (description, biogeography).  
 Doradidae gen. et sp. indet. 2 in Sánchez-Villagra and Aguilera  
 2006:215 (Table 1), 217 (Fig. 2I, caption incorrectly refers  
 to Fig. 2G,H).

*Holotype*.—UNEFM-PF-0411 (Fig. 2; cf. Fig. 3), partial left pectoral girdle with articulated pectoral-fin spine (PCS, spine incomplete, approximately distal half missing). Postcleithral process (CLE-pp) and shoulder of cleithrum (CLE-shd, portion receiving dorsal process of pectoral spine) nearly complete; dorsal limb of cleithrum (CLE-ld) incomplete and horizontal transverse limb largely missing. Partial coracoid represented by base of posterior process (COR-pp, tip missing), portion articulating with pectoral spine (COR-pvl), and part of vertical transverse limb (COR-lv) sharing suture with anterior transverse face of cleithrum; horizontal transverse limb (COR-lh) of coracoid largely missing. Maximum overall length 125.6 mm; maximum overall depth 55.5 mm. Postcleithral process dorsal length 73.5 mm; ventral length 78.5 mm; oblique length 82.5 mm; depth 30.0 mm. Locality: Urumaco Formation (middle

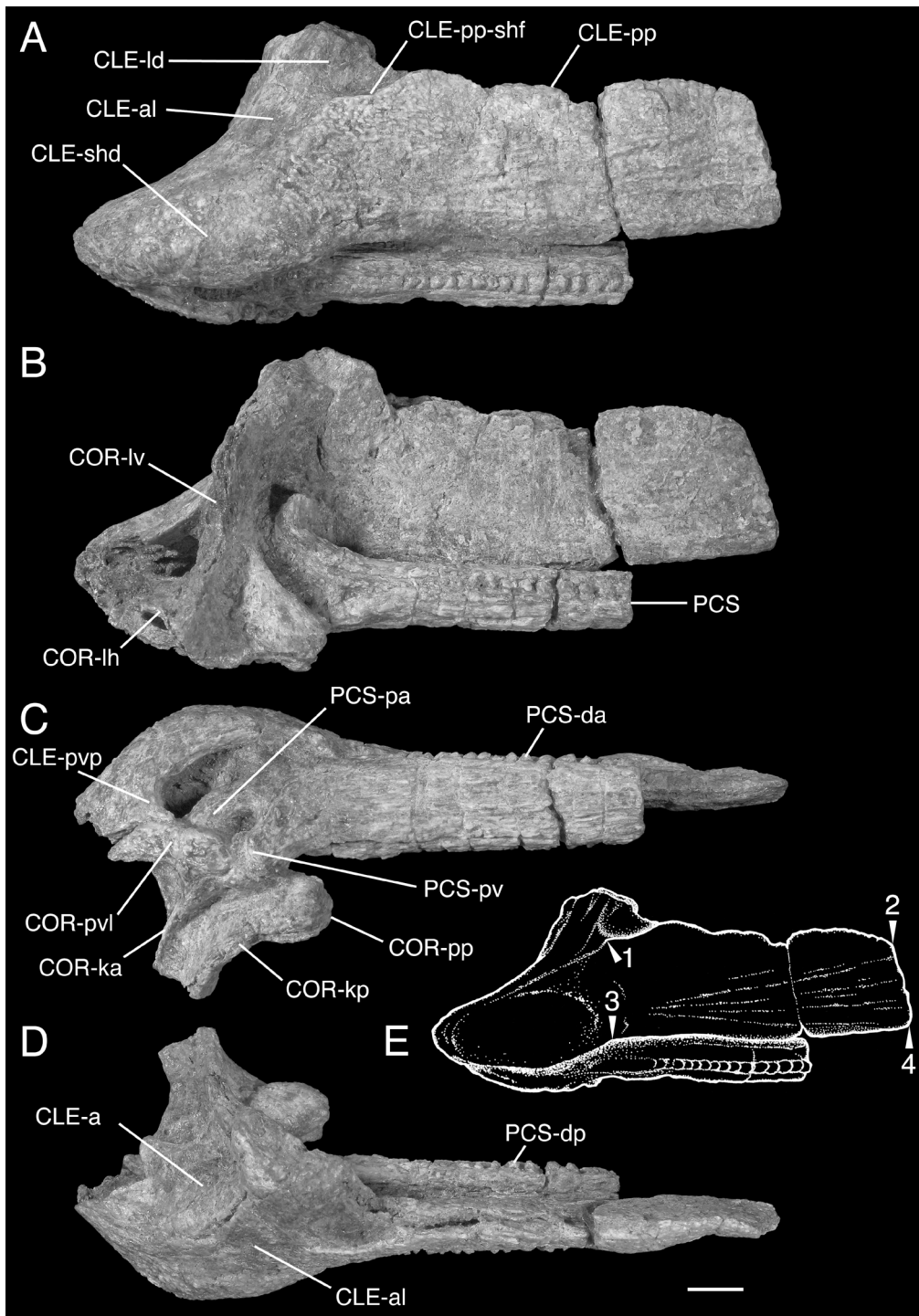


Fig. 2. Pectoral girdle and spine of *Doras dioneae* n. sp., UNEFM-PF-0411, holotype, Urumaco Formation (middle member), El Hatillo, Venezuela. A. Lateral view (left), B. Medial view, C. Ventral view, D. Dorsal view, E. Lateral view showing landmarks for select measurements. Scale bar equals 1 cm for photographs by K. Luckenbill; illustration by M. Sabaj Pérez.

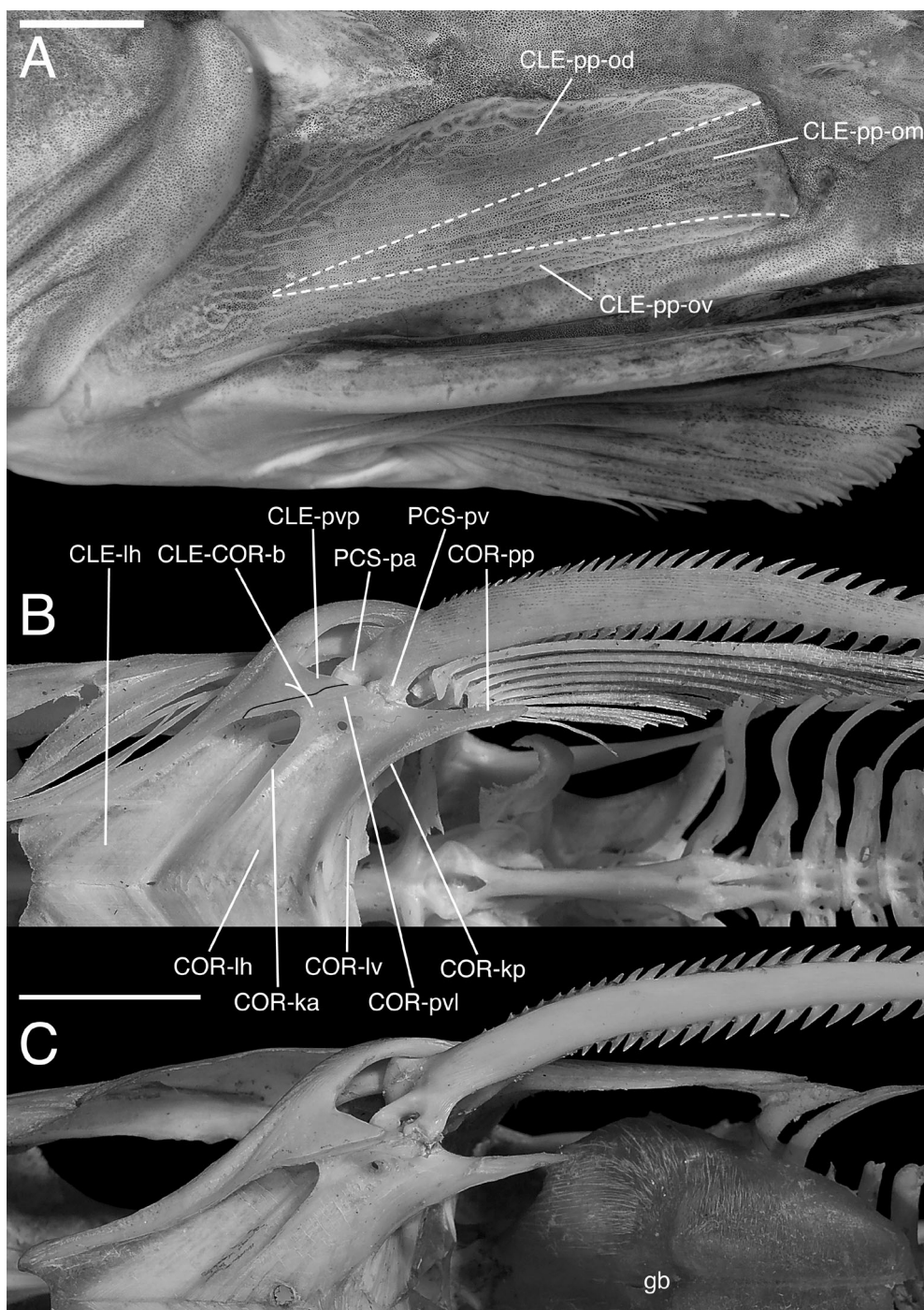


Fig. 3. Pectoral girdle and spine of modern *Doras*. A. Lateral view (left) illustrating dorsal, middle and ventral fields of ornamentation on postcleithral process of *D. carinatus*, ANSP 177275 (188 mm SL), Siparuni River, Guyana, B. Ventral view of *D. carinatus*, ANSP 180986 (170 mm SL), Essequibo River, Guyana, with CLE-COR-su outlined in black, C. Ventral view of *D. micropoetus*, ANSP 78070 (160 mm SL), Guianas. Scale bars equal 1 cm, photographs by M. Sabaj Pérez (A) and K. Luckenbill.

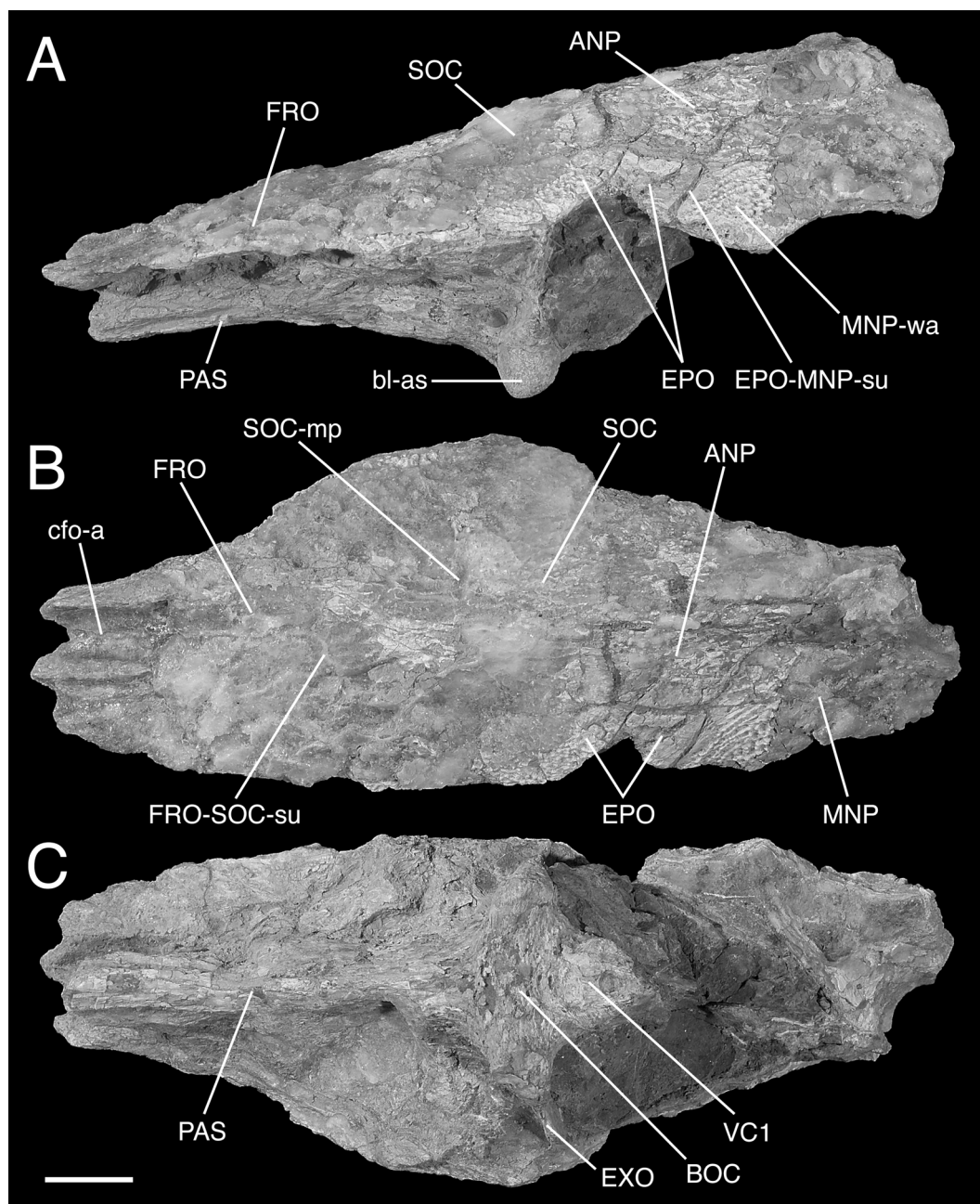


Fig. 4. Neurocranium and nuchal shield of *cf. Doras dioneae* n. sp., UNEFM-PF-0477, Urumaco Formation (upper member), Tío Gregorio, Venezuela. A. Lateral view (left), B. Dorsal view, C. Ventral view. Scale bar equals 1 cm, photographs by K. Luckenbill.

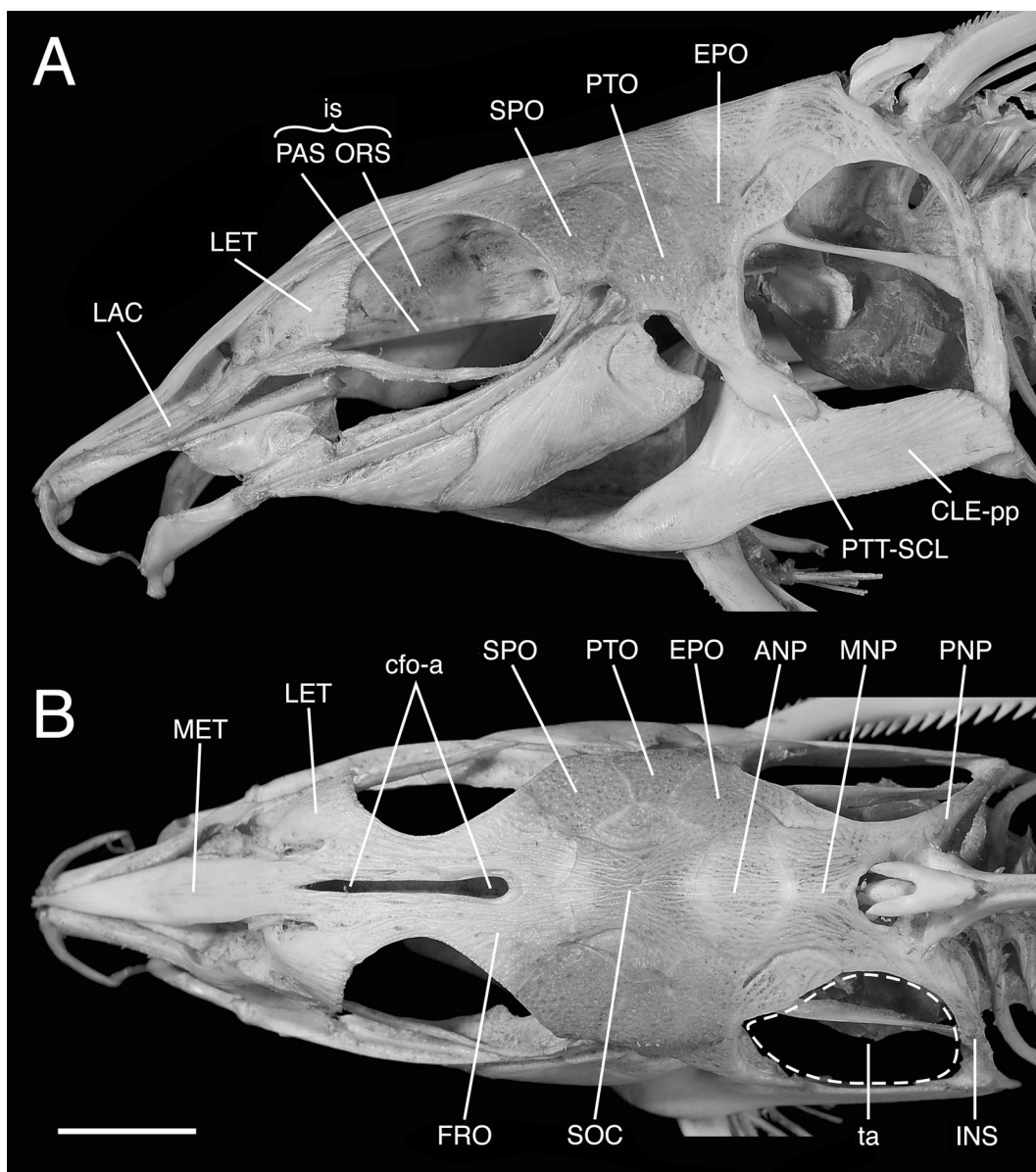


Fig. 5. Neurocranium and nuchal shield of modern *Doras micropoeus*, ANSP 78070 (160 mm SL), Guianas. A. Lateral view (left), B. Dorsal view. Scale bar equals 1 cm, photographs by K. Luckenbill.

member), El Hatillo, Quebrada Taparito, Falcón State, Venezuela.

*Non-type material.*—UNEFM-PF-0477 (Fig. 4; cf. Fig. 5), partial neurocranium and nuchal shield. Dorsally includes complete supraoccipital (SOC), nearly complete anterior nuchal plate (ANP), and portions of frontals (FRO), sphenotics, pterotics, epioccipitals (EPO) and left side of middle nuchal plate (MNP). Ventrally includes first vertebra (VC1), basioccipital (BOC), exoccipital (EXO), and partial parasphenoid (PAS, appears dorsoventrally crushed). Dorsal surface with patches of intact ornamentation. Locality: Urumaco Formation (upper member), Tío Gregorio, Falcón State, Venezuela.

*Diagnosis.*—The fossil pectoral girdle and spine is diagnosed as *Doras* by having: 1) postcleithral process (Fig. 2; cf. Fig. 3A) blade-like, subrectangular (truncated) with dorsal and ventral margins nearly parallel, posterior margin straight, weakly oblique (tilted anteriorly) and dorsal posterior corner distinct, 2) surface ornamentation of postcleithral process (Fig. 2A; cf. Fig. 3A) clearly separable into three longitudinal fields, dorsal (CLE-pp-od), middle (CLE-pp-om), ventral (CLE-pp-ov), with dorsal and middle fields nearly planar, and 3) middle field narrowly triangular with fine, elongate ridges and shallow grooves diverging gradually from point posterior to shoulder bulge to posterior margin of process. *Doras dioneae* is distinguished within *Doras* by having: 1) triangular ventral posterior process of cleithrum (Fig. 2C, CLE-pvp; cf. Figs. 3B, C) small, tip not reaching articulation of anterior process of pectoral spine (PCS-pa), 2) medial portions of anterior and posterior keels (Fig. 2C, COR-ka, COR-kp; cf. Figs. 3B, C) on ventral face of coracoid more transversely aligned, forming less than 45° angle with transverse line through body, 3) trench between coracoid keels narrow, width less than 3/4 maximum width of notch for pectoral spine insertion, and 4) medial margin of posterior coracoid keel distinctly arched and proximal to coracoid articulation with anterior process of pectoral spine.

*Description of neurocranium and nuchal shield.*—In lateral view (Fig. 4A) dorsal profile of neurocranium and nuchal shield nearly straight, moderately oblique, ascending almost continuously from frontals to posterior rim of nuchal shield. In transverse plane skull roof gently rounded across posterior portions of frontals and anterior half of supraoccipital, becoming progressively more dorsally arched, triangular towards posterior rim of nuchal shield. In dorsal view (Fig. 4B) true lateral margins of neurocranium and nuchal shield largely missing except for short, shallow concavity corresponding to lateral margin of middle nuchal plate (left side only; Figs. 4A, B). In lateral and ventral views (Figs. 4A, C) basioccipital and first vertebra removed (lowered) from dorsal surface of skull; exoccipital deep with

partial lateral portion persisting as thin transverse vertical wall spanning distance from basioccipital to skull roof, slightly angled anteroventrally; parasphenoid, narrow, moderately elevated (in ventral view), but distorted and collapsed dorsalventrally (i.e., elevation preserved in fossil less than that of original condition; Fig. 4A). Intact ornamentation on dorsal surfaces of nuchal shield and supraoccipital consisting mostly of fine network of very small, short ridges. Middorsal groove or furrow evident at least in part on posterior half of supraoccipital, obscured by adherent matrix on anterior nuchal plate.

Anterior cranial fontanelle (Fig. 4B, cfo-a) moderately wide posteriorly, elongate with parallel sides marked by elevated ridges and posterior rim rounded, contained within frontals (remote from supraoccipital) and not drawn out posteriorly as tapered sulcus. Sutures of neurocranial bones largely unclear except for that between frontals and supraoccipital (Fig. 4B, FRO-SOC-su).

Nuchal shield relatively broad (minimum width about equal to length) with moderately steep sides forming triangular transverse arch. Anterior nuchal plate (Figs. 4A, B) nearly intact, broadly pentagonal, posterior margin deeply V-shaped with posteriorly directed apex. Middle nuchal plate (Figs. 4A, B) largely incomplete; partially intact anterior wing (MNP-wa) wide and expanded anteriorly, sharing anterolaterally oblique suture with epioccipital that is collinear with suture between anterior and middle nuchal plates; remnant of lateral margin (narrowest portion of intact nuchal shield) shallowly concave (Fig. 4A).

*Description of pectoral girdle and spine.*—Postcleithral process (Fig. 2) well developed, elongate, subrectangular (truncate); dorsal and ventral margins of ornamented surface nearly parallel, posterior margin straight, weakly oblique (tilted anteriorly); all margins entire, without conspicuous dentations. Dorsal margin of process begins anteriorly at distinct point along posteriormost extent of smooth subcrescentric anterolateral face (CLE-al) of cleithrum (underlying posterior margin of opercle in life), continues posteriorly for short distance as shallow concavity elevated by distinct shelf (CLE-pp-shf) from dorsal limb of cleithrum (portion underlying posttemporal-supracleithrum in life), rises gently to form low rounded hump just posterior to dorsal cleithral limb, then continues more or less straight (ignoring chip), descending slightly before dorsal posterior corner of process (Figs. 2A, B). Ventral margin nearly straight, very gently bowed (convex) from shoulder (CLE-shd) to ventral posterior corner of process. Entire postcleithral process laterally compressed, thickness nearly uniform (i.e., blade-like), without distinct longitudinal swelling or thickening along medial face (Fig. 2D).

Lateral surface of postcleithral process ornamented with low, narrow ridges and shallow grooves; pattern of



ornamentation separable into three longitudinal fields (dorsal, middle, ventral, Fig. 2A; cf. Fig. 3A). Dorsal field (CLE-pp-od) widest anteriorly, tapering posteriorly to dorsal posterior corner; surface with small, irregular, granular ridges best developed on dorsal anterior portion. Middle field (CLE-pp-om) narrowly triangular (expanded posteriorly); surface with elongate longitudinal ridges and grooves, all of which diverge gradually from point posterior to shoulder bulge to posterior margin of process; dorsalmost ridge finishes just below dorsal posterior corner of process and ventralmost ridge finishes at ventral posterior corner. Ventral field (CLE-pp-ov) narrow, tapering posteriorly to ventral posterior corner; surface granular. Dorsal and middle fields planar, ventral field sloping medially.

Anterior transverse and anterolateral faces of cleithrum broad, smooth, the latter subcrescentic (Figs. 2A, D). Shoulder of cleithrum (CLE-shd) distinctly bulging outward. Ventral anterior rim of shoulder (Fig. 2C) with small triangular posteriorly directed process (CLE-pvp) sutured to coracoid; posterior lateral margin of same process forms apex of notch for pectoral spine; tip of process falls short of anterior process of pectoral spine (PCS-pa); anterior lateral margin of process sutured to ventral lateral process of coracoid (COR-pvl), forming cleithral-coracoid bridge (CLE-COR-b), in life distal to abductor muscles of pectoral spine.

Coracoid with deep, vertical, transverse limb (Figs. 2B, D, COR-lv) sharing long suture with anterior transverse face of cleithrum. Ventral lateral process of coracoid (Figs. 2C, COR-pvl) articulating (posteriorly) with ventral and anterior processes of pectoral spine and sutured (anteriorly) to ventral posterior process of cleithrum forming cleithral-coracoid bridge. Ventral lateral coracoid process gives rise to low, thin anterior keel (COR-ka) that projects from ventral face of horizontal limb of coracoid. Posterior process/keel and horizontal limb of coracoid largely missing. Medial margin of intact posterior keel (COR-kp) concave, forming distinct arch opposite articulation of coracoid with anterior process of pectoral spine. Anterior and posterior coracoid keels separated by narrow trench with downturned margin of posterior keel projecting more ventrally; anteriormost margin of posterior keel parallels lower anterior keel and both keels medially finish closer to transverse plane than to longitudinal.

Pectoral spine (Fig. 2) shaft depressed, subrectangular, ventral surface coarse with fine, elongate, anastomosing ridges and grooves, sides with well-preserved dentations; anterior dentations (PCS-da) along leading edge of spine blunt, weakly antrorse; posterior dentations (PCS-dp) on trailing edge blunt, slightly more narrow than anterior dentations, weakly retrorse. Anterior dentations begin near base of spine; posterior dentations begin at a distance from base slightly greater than greatest width of spine shaft. Both

anterior and posterior dentations situated in moderately deep trench flanked by ridges.

*Occurrence.*—Fossil *Doras dioneae* is known only from the Upper Miocene Urumaco Formation at El Hatillo, Quebrada Taparito and Tío Gregorio, Falcón State, Venezuela (Fig. 1).

*Etymology.*—This species is named in honor of Dione Rodrigues de Aguilera for her significant contributions to the study of Venezuelan fossil fishes.

*Comparisons of neurocranium and nuchal shield.*—The fossil neurocranium plus nuchal shield (UNEFM-PF-0477, Fig. 4) is tentatively identified as *Doras* (see Fig. 5 for modern species) based on the following shared characters, none of which are absolutely diagnostic: 1) dorsal profile nearly straight, moderately oblique, ascending almost continuously from frontals to posterior rim of nuchal shield, 2) skull roof in cross section gently rounded dorsally across posterior portions of frontals and anterior half of supraoccipital, becoming progressively more arched, triangular across nuchal shield, 3) anterior cranial fontanelle moderately wide posteriorly with rounded posterior rim contained within frontals, 4) parasphenoid and basioccipital distinctly elevated relative to skull roof in ventral view, 5) exoccipital deep, laterally with thin transverse vertical wall spanning distance from basioccipital to skull roof, 6) anterior nuchal plate wide, pentagonal, posterior margin V-shaped with posteriorly directed apex, 7) nuchal shield with shallowly concave lateral margin at narrowest point, 8) surface ornamentation with fine network of very small, short ridges, and 9) middorsal furrow or groove evident on posterior half of supraoccipital. Among nominal *Doras* the fossil neurocranium is distinguished by having: 1) basioccipital and parasphenoid moderately (vs. well) elevated in ventral view, 2) left and right vertical walls of orbitosphenoid not medially adpressed to form an interorbital septum (however, septum may have collapsed during fossil preservation), and 3) anterior wing of middle nuchal plate more extensive, suture with epioccipital deflected anterolaterally (vs. anterior wing of middle nuchal plate reduced, suture deflected posterolaterally in nominal *Doras*).

*Comparisons of pectoral girdle.*—The postcleithral (“humeral”) process is extremely well developed in doradids and contributes to a synapomorphy proposed for the family (Higuchi, 1992; de Pinna, 1998): tympanic area bounded by posttemporal-supracleithrum (anteriorly), nuchal shield (dorsally), infranuchal scute (posteriorly) and postcleithral process (ventrally) (Fig. 5). The lateral ornamented surface of the postcleithral process is variably textured and clearly distinguishable from the relatively smooth subcrescentric anterolateral face of the cleithrum that lies beneath the opercle in life. Diagnostic for many doradid genera and species are the ornamentation, thickness and shape of the

postcleithral process that varies along a continuum from lanceolate (narrow and sharply pointed) to subpolygonal (truncate) to hemi-elliptical or fan-shaped (rounded).

The shape (subrectangular, truncate) and ornamentation of the postcleithral process in the fossil is most similar to that observed in the genus *Doras* (Fig. 3A). Modern *Doras* contains two described species, *D. carinatus* (Linnaeus, 1766) and *D. micropoeus* (Eigenmann, 1912), both of which occur in coastal drainages of the Guianas (e.g., Essequibo River). There are three undescribed species of *Doras* distributed in the middle Amazon, Xingu and Tocantins, respectively. *Doras* has not been confirmed to occur in the Orinoco basin. Two species often cited in the genus *Doras*, *D. fimbriatus* and *D. punctatus*, are not closely related to true (hereafter “nominal”) *Doras* and are better treated as species *incertae sedis* in Doradidae (Sabaj and Ferraris, 2003).

In the fossil and nominal species the postcleithral process is relatively deep (vs. narrow in Amazon and Tocantins species) and has a distinctly angular dorsal posterior corner and wide, weakly oblique posterior margin (vs. rounded corner and narrower, more oblique posterior margin in Amazon and Tocantins species). In the fossil and nominal species the anterior dorsal margin of the postcleithral process presents a low rounded hump just posterior to the dorsal limb of the cleithrum (vs. dorsal margin more continuous, gently curved and shallowly convex for entire distance in Xingu species). The surface ornamentation described for the fossil process also most closely matches that of the two nominal *Doras*.

The fossil pectoral girdle is not assignable to nominal *Doras* in part because of the development of the triangular ventral posterior process of cleithrum (Fig. 2C, CLE-pvp). In nominal *Doras*, the ventral posterior process of the cleithrum is well developed with a broad base and distal tip extending beyond articulation of anterior process of pectoral spine (Figs. 3B,C, CLE-pvp). As such in modern *Doras*, the ventral posterior process of cleithrum forms much of the cleithral-coracoid bridge (at least superficially) and its lateral margin nearly completes the notch for the pectoral-spine insertion. In the fossil, the ventral posterior process of the cleithrum is relatively small, its tip falls just short of articulation of anterior process of pectoral spine, and the coracoid contributes greater proportions of cleithral-coracoid bridge and notch for pectoral-spine insertion (Fig. 2C). The condition observed in modern *Doras* (Figs. 3B,C) is typical of nearly all species of doradids with fimbriate barbels, a monophyletic group supported by morphological (Higuchi, 1992; Birindelli, 2006) and molecular (Moyer et al., 2004) data. The fossil condition is shared by a number of more basal doradid taxa with simple barbels and a few fimbriate-barbel taxa (e.g., *Trachydoras paraguayensis*, *T.*

*steindachneri*).

Additional characteristics differentiating the fossil pectoral girdle from nominal *Doras* involve the anterior and posterior keels on the ventral face of the horizontal transverse limb of coracoid (Fig. 2C, COR-ka, COR-kp). In modern nominal *Doras* the thin anterior keel (Figs. 3 B, C, COR-ka) that begins beneath the cleithral-coracoid bridge runs near and parallel to the anterior margin of the coracoid, and is strongly oblique, forming about 45° angle with transverse line through body (vs. alignment of anterior coracoid keel more transverse, forming less than 45° angle in fossil). A strongly oblique anterior coracoid keel is characteristic of nearly all doradids with fimbriate barbels. Doradids with more transversely aligned anterior coracoid keels (i.e., fossil condition) include taxa with simple barbels and a few with fimbriate barbels (e.g., *Hemidoras* spp., *Nemadoras ternetzi*). In the two modern nominal *Doras* the transition between the medial margin of the posterior coracoid keel and the transverse vertical wall of the coracoid is more gradual and remote (displaced anteriorly and medially) from the coracoid's articulation with the anterior process of the pectoral spine (Figs. 3B, C, COR-kp, COR-lv; vs. transition between medial margin of posterior coracoid keel and transverse wall of coracoid distinctly arched and located more proximal to coracoid articulation with anterior process of pectoral spine in fossil, Figs. 2B, C). Also in nominal *Doras*, the trench between the parallel keels is relatively broad, width about equal to that of notch (opening) for pectoral-spine insertion (Figs. 3B, C; vs. trench narrow in the fossil, width less than 3/4 maximum width of notch, Fig. 2C). Posterior coracoid keel with medial margin gradually curved and remote from pectoral-spine articulation, and broad trench between keels are conditions typical of fimbriate-barbel doradids and some taxa with simple barbels (e.g., *Oxydoras*). The fossil condition, on the other hand, is found in a few doradids with fimbriate barbels (e.g., some *Leptodoras*, *Nemadoras leporhinus*) and some with simple barbels.

In sum, four characteristics of the fossil (small ventral posterior process of cleithrum, arched medial margin of posterior keel proximal to pectoral-spine articulation, anterior and posterior keels more transversely aligned, trench between keels narrow) are not shared by *Doras carinatus* and *D. micropoeus* and it is unlikely (though uncertain) that they exist in the other modern undescribed *Doras*. One or more of these four fossil characteristics are shared by other doradid taxa with simple or fimbriate barbels. Modern *Doras* aside, the fossil condition for these four characteristics most closely matches those of two genera with simple barbels, *Orinocodoras* (monotypic, Orinoco endemic) and *Platyodoras* (widespread, several species). In both of these taxa, however, the postcleithral process is lanceolate with a

pointed tip, and less blade-like with a longitudinal thickening of the ventral medial face of the process.

One of the four fossil characteristics (small ventral posterior process of cleithrum) is shared by an extant species, *Trachydoras paraguayensis* (Paraná-Paraguay basin) that also has a subrectangular (truncate) postcleithral process. However, in *T. paraguayensis* the anterior portion of the postcleithral process (just posterior to the shoulder bulge) is relatively narrow, not as deep as in the fossil and modern *Doras*. Differences also are noted in the surface texture of the postcleithral process. In *T. paraguayensis* the middle field is more sharply distinguished from the dorsal and ventral fields (i.e., appears carved out) and has small anastomosing ridges (vs. middle field more planar with flanking fields and with divergent longitudinal ridges and grooves, Figs. 2A, 3A). Furthermore in *T. paraguayensis*, the posterior coracoid process is very long (posterior tip nearly even with that of postcleithral process) and robust and its ventral surface is almost completely ornamented (i.e., nearly exposed). In the fossil the posterior coracoid process is incomplete, therefore its relative length and degree of ornamentation cannot be determined.

Based on the overwhelming similarity of the fossil postcleithral process to that of the two nominal species of *Doras*, and the gross dissimilarity of the fossil process to other taxa sharing somewhat more labile characteristics of the coracoid keels and ventral posterior cleithral process, the fossil pectoral girdle is referred to the genus *Doras*. Although we rule out assignment of the fossil pectoral girdle to *Trachydoras*, future comparisons of more complete fossil material should include this taxon, particularly *T. paraguayensis*. The fossil pectoral girdle is not assignable to nominal *Doras* and, therefore, described as a new species.

*Doraops* cf. *zuloagai* Schultz, 1944  
Figs. 6, 8A, 9A–D

cf. *Rhinodoras* sp. in Aguilera 2004:63 (description, biogeography).

*Doradidae* gen. et sp. indet. 1 in Sánchez-Villagra and Aguilera 2006:215 (Table 1), 217 (Fig. 2F).

**Material.**—All Urumaco Formation (upper member), Tío Gregorio, Falcón State, Venezuela: UNEFM-PF-0271 (Fig. 6; cf. Fig. 7), nearly complete neurocranium, nuchal shield, anterior vertebrae and dorsal-fin base; two major moieties separated across anterior nuchal plate (ANP) and epioccipitals (EPO). Anterior moiety lacking marginal portions of sphenotics (SPO), frontals (FRO) and mesethmoid (MET); ventrally includes first vertebrae, basioccipital (BOC) and exoccipital including their lateral processes (os-

sified transcapular ligament gone) plus complete parasphenoid (PAS) and portions of prevomer, lateral ethmoids (LET) and orbitosphenoid (ORS). Smaller posterior moiety dorsally includes portions of anterior, middle (MNP) and right posterior (PNP) nuchal plates and remnants of articulated dorsal locking spine (DLS) and anterior radials; ventrally includes remnants of Weberian complex (wc) and proximal radials of dorsal fin. All surfaces badly eroded, only small remnants of ornamentation persist on dorsal surfaces. Maximum preserved overall length when assembled 173.5 mm. UNEFM-PF-0415 (Fig. 8A; cf. Fig. 8B), partial neurocranium and nuchal shield. Dorsally includes partial frontals (portion just posterior to anterior cranial fontanelle), sphenotics and pterotics (left side nearly complete), epioccipitals (complete or nearly so), supraoccipital and anterior nuchal plate (complete), partial middle nuchal plate, posterior nuchal plates (left intact, right detached, both complete or nearly so), and articulated remnants of dorsal locking spine and anterior radials. Ventrally includes basioccipital and exoccipital including their lateral processes (ossified transcapular ligament gone) and posterior portion of parasphenoid. Most surfaces largely eroded except some ornamentation intact on nuchal shield. Maximum preserved overall length 116 mm. UNEFM-PF-0278 (Figs. 9A–D; cf. Fig. 9E–G), partial left pectoral girdle with articulated pectoral spine (spine incomplete, approximately distal half missing). Cleithrum with postcleithral process and “shoulder” (portion receiving dorsal process of pectoral spine) complete; dorsal limb nearly complete (missing tip of dorsal process); horizontal transverse limb largely incomplete (only basal portion remaining). Partial coracoid represented by base of posterior process (tip missing) and keel, portion articulating with pectoral spine, and vertical transverse limb sharing suture with anterior transverse face of cleithrum; horizontal transverse limb of coracoid missing. Maximum preserved overall length 91.3 mm. Postcleithral process ventral length 48.2 mm; depth 18.5 mm. UNEFM-PF-0413, partial left pectoral girdle with articulated pectoral spine (spine incomplete, approximately distal third missing). Cleithrum with “shoulder” complete, dorsal limb nearly complete (eroded, missing tip of dorsal process); postcleithral process and horizontal transverse limb largely missing (only basal portions remaining). Partial coracoid represented by base of posterior process (tip missing) and keel, portion articulating with pectoral spine, and portion of vertical transverse limb sharing suture with anterior transverse face of cleithrum; horizontal transverse limb of coracoid partially complete (missing anterior and symphyseal portions). Maximum preserved overall length 107.2 mm.

**Description of neurocranium and nuchal shield.**—In lateral view (Fig. 6A) neurocranium with dorsal profile nearly straight, weakly oblique from posterior mesethmoid

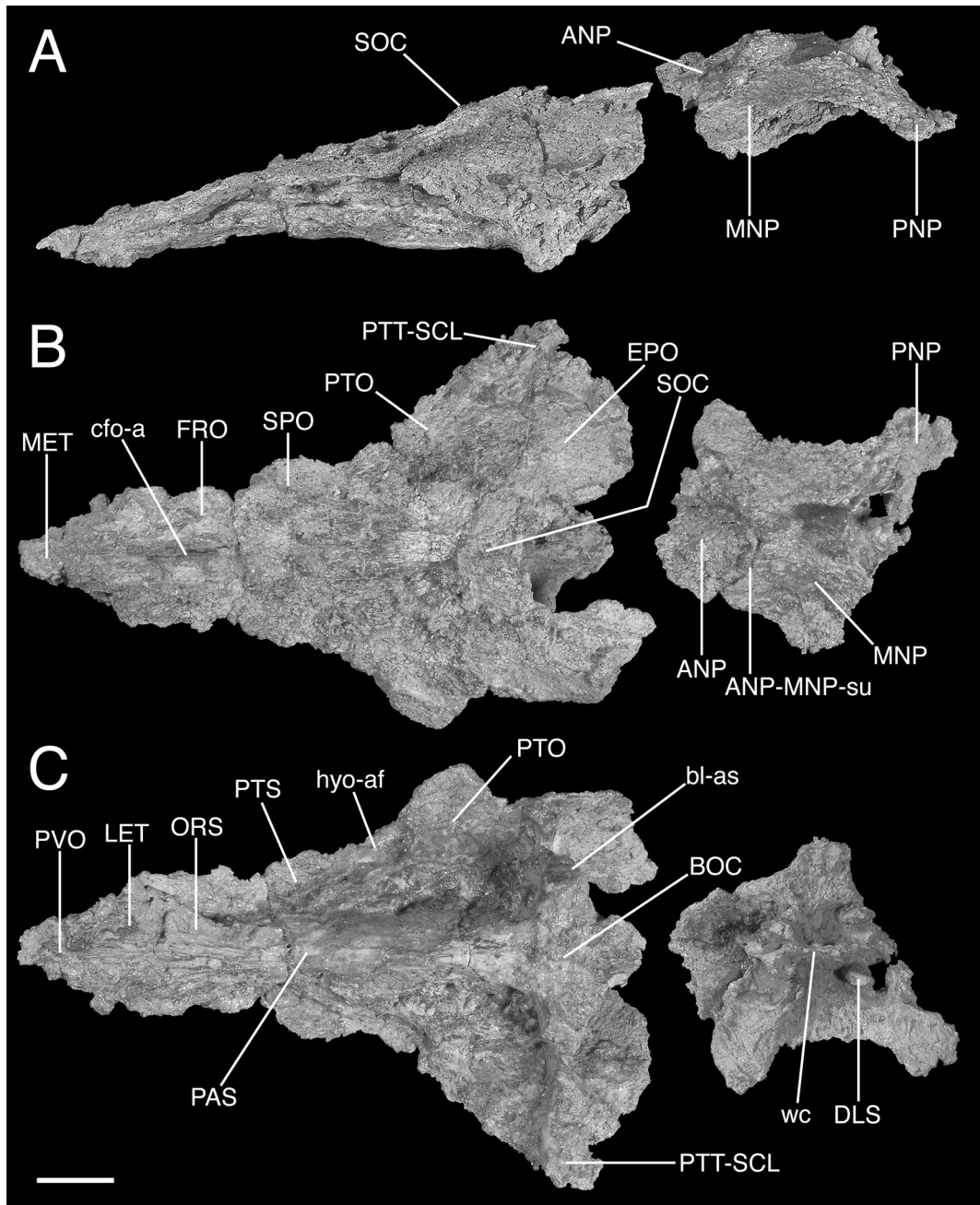


Fig. 6. Neurocranium and nuchal shield of fossil *Doraops cf. zuloagai*, UNEFM-PF-0271, Urumaco Formation (upper member), Tío Gregorio, Venezuela. A. Lateral view (right), B. Dorsal view, C. Ventral view. Scale bar equals 1 cm, photographs by K. Luckenbill.

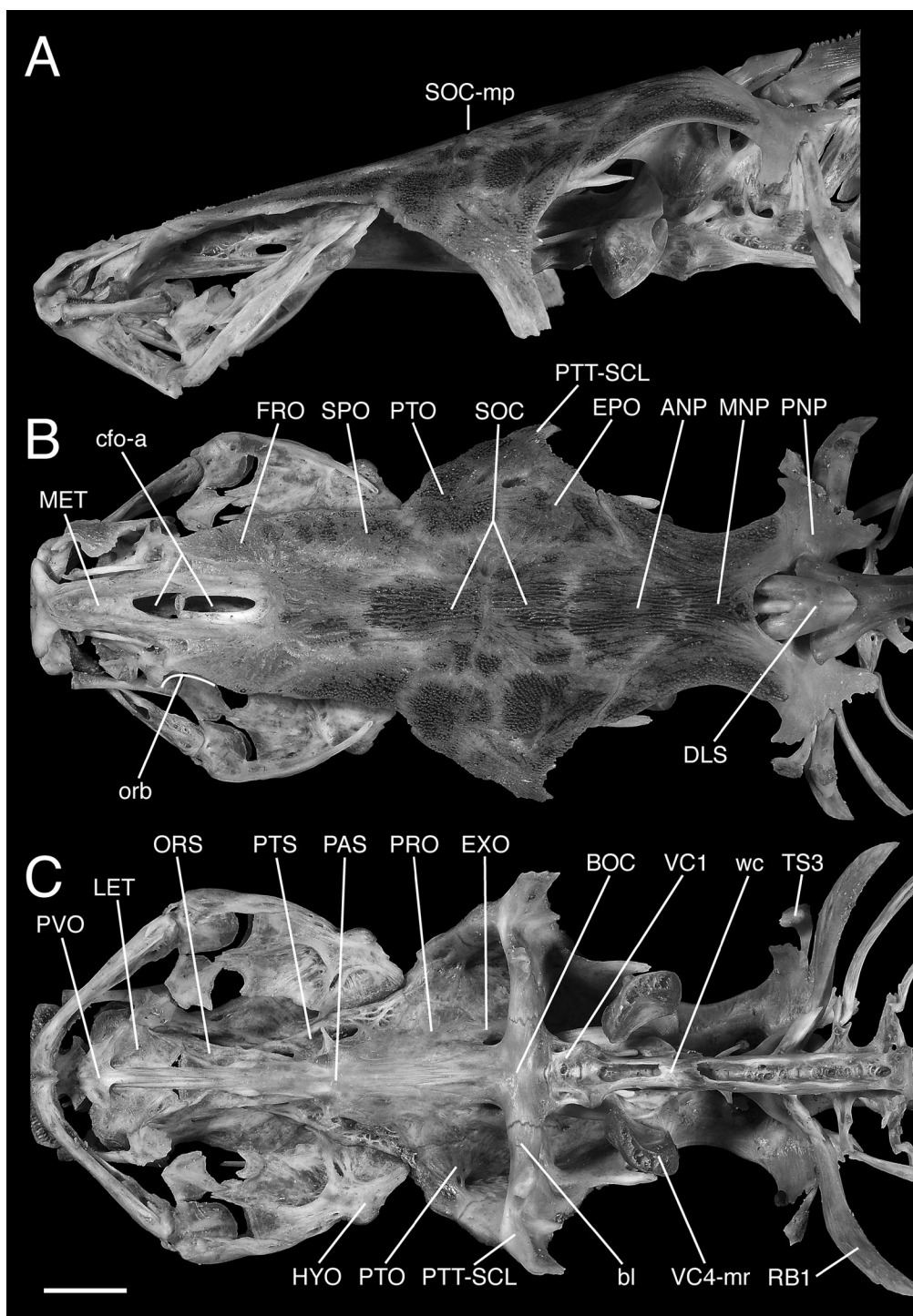


Fig. 7. Neurocranium and nuchal shield of modern *Doraops zuloagai*, ANSP 179558 (256 mm SL), Río Catatumbo, Venezuela. A. Lateral view (left), B. Dorsal view, C. Ventral view. Scale bar equals 1 cm, photographs by K. Luckenbill.

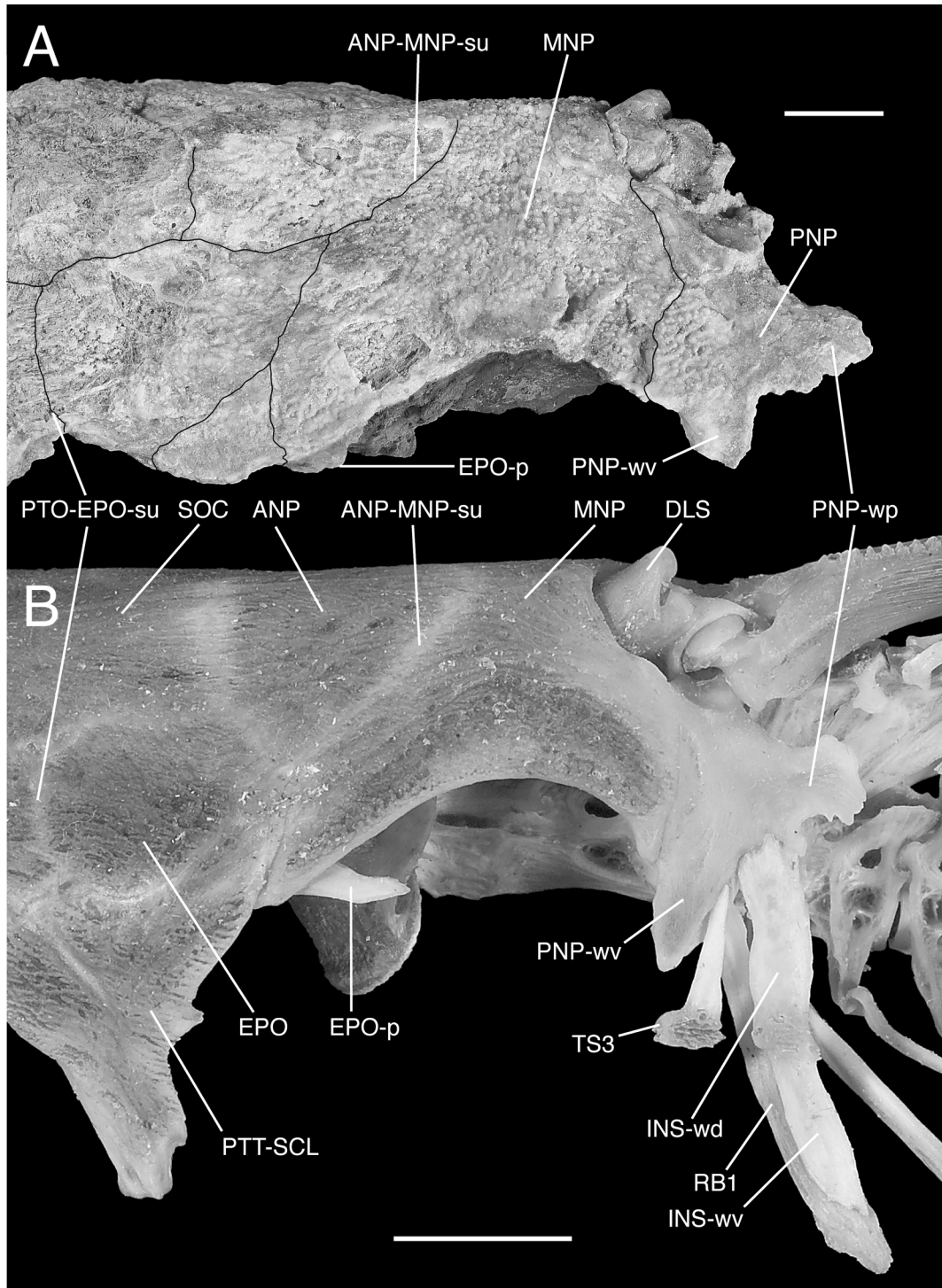


Fig. 8. Posterior neurocranium and nuchal shield of *Doraops*. A. Lateral view (left) of fossil *D. cf. zuloagai*, UNEFM-PF-0415, Urumaco Formation (upper member), Tío Gregorio, Venezuela, with sutures outlined in black, B. Lateral view (left) of modern *D. zuloagai*, ANSP 179558 (245 mm SL), Río Catatumbo, Venezuela. Scale bars equal 1 cm, photographs by K. Luckenbill.

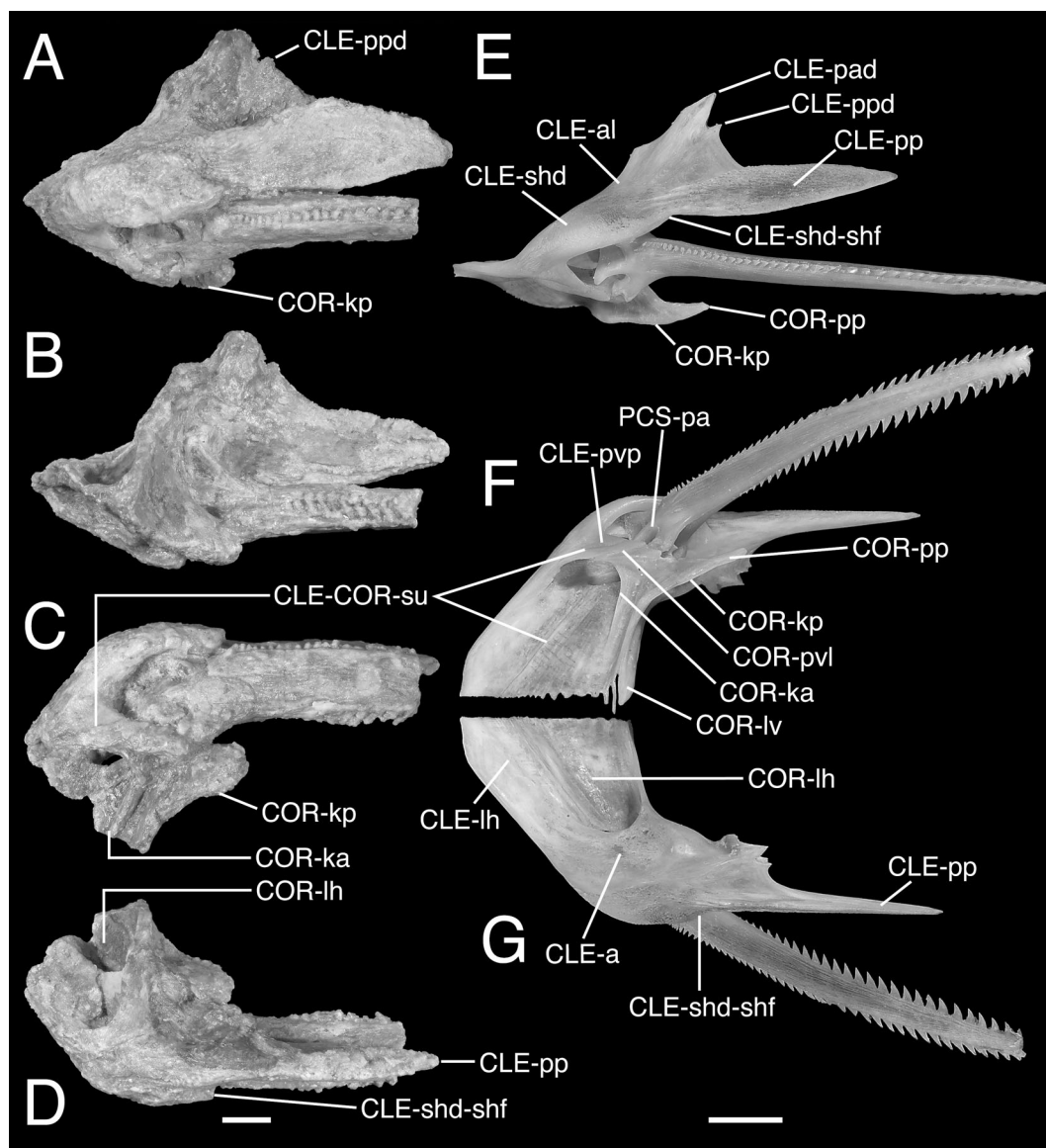


Fig. 9. Pectoral girdle and pectoral-fin spine of fossil (A–D) *Doraops cf. zuloagai*, UNEFM-PF-0278, Urumaco Formation (upper member), Tío Gregorio, Venezuela, and modern (E–F) *D. zuloagai*, ANSP 179558 (245 mm SL), Río Catatumbo, Venezuela. A. Lateral view (left), B. Medial view, C. Ventral view, D. Dorsal view, E. Lateral view (left), F. Ventral view, G. Dorsal view. Scale bars equal 1 cm, photographs by K. Luckenbill.

to anterior portion of supraoccipital, and from posterior portion of supraoccipital to posterior rim of nuchal shield; posterior dorsal profile parallel to and in plane slightly elevated from anterior profile by gentle inflection at center of supraoccipital (middle pitline). In transverse plane, dorsal surface flattened anteriorly across frontals; gently arched, broadly rounded across pterotics and anterior supraoccipital; progressively more arched, broadly subtriangular, from middle pitline of supraoccipital to posterior rim of nuchal shield. In dorsal view (Fig. 6B) neurocranium roughly triangular with concave sides converging anteriorly to tip (i.e., posterior portion of remaining mesethmoid) and diverging posteriorly towards temporal region (lateralmost rim of posttemporal-supracleithrum, PTT-SCL); nuchal shield butterfly-shaped with relatively smooth, moderately deep concave sides corresponding to lateral margins of middle nuchal plate. In ventral view (Fig. 6C) parasphenoid weakly expanded anteriorly and moderately elevated relative to dorsal surface of skull in ventral view. Intact ornamentation on dorsal surface fine; mostly granular and pitted on middle nuchal plate; more striated with irregular, weakly anastomosing longitudinal ridges on anterior nuchal plate; no evidence of middorsal groove or furrow on nuchal shield.

Anterior cranial fontanelle (cfo-a) narrowly elliptical, slit-like, not extending posteriorly beyond a line across anteriormost portions of sphenotics (however, anteriormost tips of sphenotics appear to be missing); fontanelle bordered largely by frontals (posteriorly) and in small part by mesethmoid (anteriorly). Sulcus surrounding anterior cranial fontanelle scarcely evident (surfaces of mesethmoid and frontals badly eroded); longitudinal ridges flanking sulcus also scarcely evident (portion of ridge evident on left side in UNEFM-PF-0271). Frontals (FRO) flattened, margins not intact. Sphenotics (SPO) nearly planar, elongate, tapered anteriorly; lateral margins shallowly sinuous, concave posteriorly, convex anteriorly (Fig 6B).

Temporal region subtriangular with large, medial margins of pterotic (PTO) and epioccipital (EPO) forming base and posttemporal-supracleithrum (PTT-SCL) forming rounded apex. Pterotic sharing sutures with sphenotic (anteriorly), supraoccipital (medially), epioccipital (posteriorly) and posttemporal-supracleithrum (posterolaterally). Epioccipital sharing sutures with pterotic (anteriorly), supraoccipital and anterior nuchal plate (medially), middle nuchal plate (posteriorly) and posttemporal-supracleithrum (laterally); base of posteriorly directed process evident in UNEFM-PF-0415 (Fig. 8A, EPO-p).

Nuchal shield relatively long and broad (minimum width slightly greater than length in UNEFM-PF-0415); sides oblique, forming transverse, subtriangular arch (Fig. 8A); middorsal longitudinal groove not evident; nuchal foramina absent. Anterior nuchal plate (ANP) roughly pen-

tagonal, posterior margin V-shaped with posteriorly directed apex. Middle nuchal plate (MNP) butterfly-shaped with lateral margins moderately concave. Posterior nuchal plate (PNP) subtriangular; distal margins expanded posteriorly and ventrally into separate, wing-like apices; surfaces of wings relatively smooth except for patch along suture with middle nuchal plate where ornamentation is similarly granular and pitted. Posterior ventral margin of posterior nuchal plate (between ventral and posterior apices) irregular with triangular cut that in life presumably received dorsalmost tips of dorsal wings of infranuchal scute (Fig. 8B, INS-wd) and third tympanal scute (TS3).

*Description of pectoral girdle and spine.*—Postcleithral process (Fig. 9A–D) moderately developed, subdiamond-shaped with acute distal tip (bluntly pointed); margins more or less entire, without conspicuous dentations; dorsal margin broadly roof-shaped with rounded central apex just distal to posterior margin of dorsal limb of cleithrum; anterior half of dorsal margin forming long, strong shelf with dorsal limb of cleithrum; ventral margin more gently bowed, convex. Entire postcleithral process laterally compressed, slightly tilted ventromedially; lateral surface planar, medial surface slightly more swollen with subventral longitudinal thickening. Lateral surface of postcleithral process ornamented with low, fine longitudinal ridges and shallow grooves (anterior third) transitioning to fine granulations (posterior two-thirds). Surface ornamentation not clearly separable into longitudinal fields and without raised, longitudinal carina.

Anterior and anterolateral faces of cleithrum very broad and gently sloping, smooth, subcrescentric (Figs. 9A, E, G, CLE-a, CLE-al). Intact portion of dorsal limb of cleithrum (lying below posttemporal-supracleithrum in life) subtriangular with a broad, weakly-sloped base (ascending posteriorly), oblique sides and blunt dorsal apex (dorsal tip presumed missing); anterior portion of dorsal limb obliquely thickened, posterior portion (between oblique thickening and strong shelf formed by dorsal margin of postcleithral process) thinner, oblique posterior margin nearly straight and entire except for small subtriangular jag (barb, probable remnant of posterior dorsal process, CLE-ppd, Figs. 9A, E) closer to apex of remaining dorsal limb than to its posterior base.

Shoulder of cleithrum distinctly bulging, inflated; transition to postcleithral process relatively abrupt, marked by shallow shelf ventrally (Fig. 9A; cf. Fig. 9E, CLE-shd-shf). Ventral rim of anterior shoulder with triangular posterior process sutured to coracoid (CLE-pvp); same process with posterior lateral margin forming apex of notch for pectoral spine, tip falling just short of anterior process of pectoral spine (PCS-pa), and anterior lateral margin sutured to ventral lateral process of coracoid (COR-pvl), forming cleithral-



coracoid bridge.

Coracoid with short transverse vertical limb sharing oblique suture with anterior face of cleithrum. Ventral lateral process of coracoid (COR-pvl) articulating (posteriorly) with ventral and anterior processes of pectoral spine and sutured (anteriorly) to ventral posterior process of cleithrum (CLE-pvp) forming cleithral-coracoid bridge. Ventral lateral coracoid process gives rise to low, thin, oblique anterior keel (COR-ka) that projects from ventral face of transverse horizontal limb of coracoid. Cleithral-coracoid bridge relatively long, enclosing broad low tunnel through which in life passed spine-abductor muscles originating on ventral surface of horizontal limb of coracoid. Continuous subtriangular arch formed by anterior margin of cleithral-coracoid bridge and anterior keel on ventral surface of coracoid.

Posterior coracoid process (COR-pp) incomplete (posterior tip missing). Medial margin of posterior keel (COR-kp) concave, forming shallowly rounded arch opposite articulation of coracoid with anterior process of pectoral spine. Anterior and posterior coracoid keels separated by a narrow trench with downturned medial margin of posterior keel projecting more ventrally; anteriormost margin of posterior keel parallels low anterior keel and both keels are angled anteromedially at about a 45° angle.

Pectoral spine shaft (Fig. 9A–D) depressed, rectangular, ventral surface coarse with elongate and anastomosing ridges and grooves, sides with well-preserved dentations; anterior dentations (leading edge of spine) more rounded than sharp, erect except distalmost weakly antrorse; posterior dentations (trailing edge) weakly pointed, triangular (width of base more than twice that of anterior dentations), distinctly retrorse. Anterior dentations begin at base of spine. Posterior dentations begin at a distance from base about equal to depth of proximal spine shaft. Both anterior and posterior dentations situated in trench flanked by ridges.

*Comparisons of neurocranium and nuchal shield.*—The neurocranium and nuchal shield in fossil and modern *Doraops* (Figs. 6–8) share a combination of characteristics putatively diagnostic among Doradidae: 1) dorsal profile of neurocranium nearly straight, weakly oblique from posterior mesethmoid to anterior portion of supraoccipital, and from posterior portion of supraoccipital to posterior rim of nuchal shield, the latter profile paralleling anterior profile in plane slightly elevated by gentle inflection at middle pitline of supraoccipital, 2) transverse plane of dorsal surface flattened anteriorly across frontals, gently arched, broadly rounded across pterotics and anterior supraoccipital, and becoming progressively more arched, broadly subtriangular, from middle pitline of supraoccipital to posterior rim of nuchal shield, 3) sphenotics elongate, tapered anteriorly, 4) posterior nuchal plate subtriangular, expanded

posteriorly and ventrally into separate, wing-like apices, 5) posterior nuchal plate with smooth posterior wing, 6) nuchal shield relatively broad, minimum width > 84.2% of length, 7) lateral margins of middle nuchal plate moderately convex, 8) middorsal nuchal groove absent or scarcely evident and incomplete, and 9) nuchal foramina absent.

The absence of paired foramina in the fossil nuchal shield rules out most fimbriate genera of Doradidae. Fimbriate-barbel doradids without nuchal foramina are distinguished by having a posterior nuchal plate that is relatively narrow, vertically elongate (at times rib-shaped; e.g., Fig. 5) and lacks the posterior wing-like expansion and subtriangular shape characteristic of fossil and modern *Doraops*. Furthermore, in some fimbriate-barbel doradids without nuchal foramina (e.g., *Doras*, *Leptodoras* and *Trachydoras*) the skull is deeper, more compressed; the parasphenoid is narrow and extremely well elevated relative to the dorsal plane of skull in ventral view; and the left and right vertical walls of orbitosphenoid are deep and thin, compressed (*Trachydoras*) or adpressed as medial interorbital septum (*Doras* and *Leptodoras*; Fig. 5A). In the fossil and modern *Doraops* the parasphenoid is moderately elevated in ventral view and the vertical walls of orbitosphenoid are remote, not forming median interorbital septum.

Doradids with simple barbels tend to have more depressed heads (*Oxydoras*, *Rhinodoras* and *Rhynchodoras* excepted) as in the fossils. Most simple-barbel doradids can be distinguished from the fossils by having posterior nuchal plate with posterior wing-like expansion distinctly ornamented. Simple-barbel doradids having posterior nuchal plate with posterior wing smooth include: *Centrodoras* (three modern species, one of which is undescribed), *Doraops* (monotypic), *Lithodoras* (monotypic), *Megalodoras* (two modern species) and *Pterodoras* (two modern species). *Lithodoras* is distinguished from fossil and modern *Doraops* by having nuchal shield with middorsal groove distinct, complete from middle pit-line of supraoccipital to posterior rim of nuchal shield. In modern *Doraops* the middorsal groove is scarcely evident and incomplete, not reaching suture between anterior and middle nuchal plates. In the fossil the middorsal groove is certainly absent from the middle nuchal plate (surface intact), and there is no evidence of a middorsal groove on the anterior nuchal plate (surface largely intact).

In *Megalodoras* the lateral margins of the nuchal shield are more strongly concave, tracing a higher and tighter arc above the tympanic region. Furthermore, *M. uranoscopus* (Amazon basin) has a distinct and complete middorsal groove. In *M. guayoensis* (Orinoco basin) the middorsal groove is distinct and complete in juveniles, but lacking in adults (SL > 350 mm). *Megalodoras guayoensis* (n=4, SL 141–408 mm) is distinguished from modern and fossil

*Doraops* by having a relatively narrow nuchal shield, minimum width 64.9–79.2% of length compared to 84.2–89.4% of its length in modern *Doraops* (n=3, SL 245–277 mm) and greater than 100% in fossil (UNEFM-PF-0415).

*Centrodoras* is similarly distinguished from fossil and modern *Doraops* by having a relatively narrow nuchal shield, minimum width 55.3–76.1% of length (n=15, SL 104–302 mm) with strongly concave lateral margins. Furthermore, in *C. hasemani* and the undescribed species (both Negro basin) the middorsal groove is distinct and complete or nearly so (i.e., extending at least to suture between anterior and middle nuchal plates). In *C. brachiatus* (Amazon basin) the middorsal groove is present but less distinct and ranges from complete (juveniles) to incomplete (finishing before suture between anterior and middle nuchal plates) in adults. It is also noted that in *Centrodoras* and sometimes *Megalodoras* the anteriormost free margin of the sphenotic contains a distinct corner that posteriorly completes the shallow concavity of the orbital rim. In modern *Doraops* the sphenotic does not contribute the orbital rim as this shallow concavity is completed within the lateral margin of the frontal. The condition in fossil *Doraops* is unclear because the anterior margins of the sphenotics appear to be missing.

*Pterodoras* is sister to *Doraops* based on morphological (Higuchi, 1992; Birindelli, 2006) and molecular (Moyer et al., 2004) evidence. *Pterodoras* is distinguished in part by having posterior nuchal plate with posterior wing relatively shorter and deeper, free margin broadly rounded, and ventral wing slender, elongate, curving anteriorly. Furthermore, in *Pterodoras* the nuchal shield is slightly narrower, minimum width 58.6–66.2% of length in *P. granulatus* (Amazon and Paraná-Paraguay basins, n=6, SL 128–346 mm) and 70.6–83.5% of length in *P. rivasi* (Orinoco basin; n=5, SL 139–425 mm).

*Comparisons of pectoral girdle.*—The following combination of characteristics of the pectoral girdle shared by fossil and modern *Doraops* (Fig. 9) is putatively diagnostic among Doradidae: 1) anterior and anterolateral faces of cleithrum very broad, gently sloping, 2) postcleithral process sub-diamond shaped with anterior base significantly more shallow than greatest depth, margins entire, dorsal margin broadly roof-shaped with rounded central apex, ventral margin gently bowed (convex), lateral surface planar (without longitudinal carina) and ornamented with fine, low ridges, shallow grooves and small granulations not separable into distinct longitudinal fields, 3) transition from shoulder to postcleithral process rather abrupt, marked by shallow shelf ventrally (CLE-shd-shf), 4) triangular ventral posterior process of cleithrum with tip falling just short of anterior process of pectoral spine, 5) cleithral-coracoid bridge long and forming broad low tunnel for passage of muscles in life, 6) medial margin of posterior coracoid keel

concave, and 6) anterior medial portions of anterior and posterior coracoid keels proximal, parallel, and angled anteromedially.

The foregoing combination of features is most closely approximated by *Orinocodoras* and *Rhinodoras*, the latter cited as a preliminary identification of the same fossil in Aguilera (2004:63). In *Orinocodoras* and *Rhinodoras* the postcleithral process differs by having: 1) dorsal margin steeply arched with higher, angular apex (vs. shallow rounded apex in *Doraops*), 2) exposed ventral margin more linear (vs. gently bowed, convex), and 3) exposed surface often with longitudinal ridge or low carina (vs. planar).

A minor discrepancy between the fossil and modern *Doraops zuloagai* is the ventral length to depth ratio of the postcleithral process (Appendix 3). The fossil process is rather stout (ventral length/depth 2.6) whereas in modern *Doraops* the process is more elongate and attenuate (length/depth ranging from 4.1–5.0). The length/depth ratio steadily decreases with size in the three modern *Doraops* measured (SL 245–277 mm). Based on pectoral spine width and depth, the SL of the fossil fish is estimated to be 690–770 mm, 2.5–2.8 times that of the largest modern *Doraops* measured. The length/depth ratio of the fossil postcleithral process may reflect ontogenetic changes consistent with modern *Doraops* or it may be diagnostic of a new species of *Doraops*.

It is noted that the pectoral girdle in large specimens of *Lithodoras dorsalis* (Amazon basin) share a number of similarities with the fossil and modern *Doraops*, particularly with respect to the postcleithral process. However, in *Lithodoras* the deepest part of the postcleithral process is equal to or barely deeper than its anterior base (taken at vertical through posterior ventral margin of “shoulder” bulge (vs. base of postcleithral process relatively shallow, distinctly more so than its deepest part in fossil and modern *Doraops*). Furthermore, the dentations along the anterior and posterior margins of the pectoral spine increase in size and spacing more dramatically in *Lithodoras*.

*Rhinodoras cf. thomersoni* Taphorn and Lilyestrom, 1984 (Figs. 10, 12A, 13A,B,D,E)

*Oxydoras* sp. in Aguilera 2004:60–61 (description, biogeography).

Doradidae gen. et sp. indet. 1 in Sánchez-Villagra and Aguilera 2006:215 (Table 1), 217 (Fig. 2D,E).

*Material.*—UNEFM-PF-0157 (Figs. 10, 12A; cf. Figs. 11, 12B), nearly complete neurocranium, nuchal shield, anterior vertebrae and dorsal-fin base; two moieties separated across anterior nuchal plate (ANP) and epioccipitals (EPO). Anterior moiety lacking marginal portions of sphenotics (SPO) and frontals (FRO); lateral ethmoids and mesethmoid

largely gone; ventrally includes basioccipital (BOC), exoccipital, ossified transcapular (Baudelot's) ligament (bl) and parasphenoid (PAS) to point level with suture between orbitosphenoid and lateral ethmoid (anterior half of parasphenoid broken but attached and offset from posterior half). Smaller posterior moiety dorsally includes middle nuchal plate (MNP, nearly complete), partial posterior nuchal plate (PNP), articulated dorsal locking spine (DLS, complete including ventral processes), and remnants of anterior radials; ventrally with portion of Weberian complex (wc) and proximal radials of dorsal fin. All surfaces largely eroded except some ornamentation intact on nuchal shield and temporal region. Maximum preserved overall length 149 mm. Locality: Urumaco Formation (middle member), Las Huertas, Falcón State, Venezuela. UNEFM-PF-0478 (Figs. 13 A, B, D, E; cf. Fig. 13C), partial cleithrum including shoulder bulge (complete), anterolateral face, basal portion of dorsal limb (tip missing), and basal portion of postcleithral process (distal portion largely missing); ornamentation largely intact. Maximum length 78.3 mm; maximum depth 49.7 mm). Locality: Urumaco Formation (upper member), Tío Gregorio, Falcón State, Venezuela.

*Description of neurocranium and nuchal shield.*—In lateral view (Fig. 10A) dorsal profile of neurocranium very gently rounded (convex) anteriorly, rising gently from interorbital region to supraoccipital, then more steeply at distinct inflection just posterior to frontal-supraoccipital suture, presumably leveling off posteriorly along anterior nuchal plate (across which fossil is broken) and finishing horizontal from suture between anterior and middle nuchal plates to posterior rim of nuchal shield. In transverse plane, dorsal surface flattened anteriorly across frontals and sphenotics, gently arched, broadly rounded across pterotics and anterior portion of supraoccipital; arch becoming progressively more distinct at inflection, broadly triangular, from middle pitline of supraoccipital (SOC-mp) to nuchal region and steepest posteriorly, across middle nuchal plate (sides strongly oblique). In dorsal view (Fig. 10B) neurocranium roughly triangular with concave sides converging anteriorly to tip (corresponding to anterior frontals, mesethmoid missing) and diverging posteriorly towards temporal region (lateralmost rim of posttemporal-supracleithrum); nuchal shield butterfly-shaped with relatively smooth, deeply concave sides corresponding to lateral margins of middle nuchal plate. In ventral view (Fig. 10C) parasphenoid moderately elevated relative to dorsal surface of skull (in ventral view) and distinctly expanded anteriorly with raised anterior margins. Ossified transcapular (Baudelot's) ligaments (bl), paired transverse spans between lateral processes of basioccipital and exoccipital medially and posttemporal-supracleithrum laterally, with robust ventral projections (bl-pv) slightly deflected posteriorly and

subtriangular in posterior view (Fig. 12A; cf. Fig. 12B). Ventral medial margins of projections oblique, forming broad subtriangular arch with ventral face of basioccipital as its rounded apex; lateral margins of each projection are shorter, more vertical, forming tight rounded arch with the medial wall of the posttemporal-supracleithrum. Intact ornamentation on dorsal surface of pterotics, epioccipitals and lateral portions of supraoccipital mostly fine, granular or with short, irregular ridges; medial portions of supraoccipital and nuchal shield more striated with irregular, longitudinal ridges; presence of middorsal groove or furrow on anterior and middle nuchal plates unclear.

Posterior portion of anterior cranial fontanelle (cfo-a) narrowly elliptical, slit-like, enclosed by frontals (anterior portion of fontanelle missing). Anterior cranial fontanelle not extending posteriorly beyond plane level with anteriormost tips of sphenotics. Narrow sulcus surrounding posterior portion of anterior cranial fontanelle barely evident, flanked by narrow longitudinal ridges. Frontals (FRO) flattened, lateral margins largely missing; sphenotics (SPO) planar, moderately elongate, tapered anteriorly.

Each side of temporal region subtriangular with large pterotic (PTO) and epioccipital (EPO) forming base and posttemporal-supracleithrum (PTT-SCL) forming rounded apex deflected posteriorly. Pterotic sharing sutures with sphenotic (anteriorly), supraoccipital (medially), epioccipital (posteriorly) and posttemporal-supracleithrum (posterolaterally). Epioccipital sharing sutures with pterotic (anteriorly), supraoccipital (medially), anterior and middle nuchal plates (posteriorly) and posttemporal-supracleithrum (laterally).

Anterior nuchal plate (ANP) largely missing due to break; presumably with triangular posterior apex based on intact anterior margin of middle nuchal plate. Middle nuchal plate (MNP) butterfly-shaped with lateral margins strongly concave and strongly oblique sides forming steep triangular transverse arch. Posterior nuchal plate (PNP) incomplete; subtriangular, expanded posteriorly and ventrally; ventral expansion rounded, extending only slightly beyond suture with middle nuchal plate; posterior expansion wing-like, more triangular with apex directly posteriorly.

*Description of pectoral girdle.*—Postcleithral process (Figs. 13A, B, D, E) with deep base (maximum depth 37.4 mm); basal remnant laterally compressed, blade-like, with thickness nearly uniform, greatest subventrally; ventral edge rounded with evidence of low, narrow, medial ridge (CLE-pp-rv) that continues anteriorly onto posterior ventral surface of shoulder bulge of cleithrum (CLE-shd); dorsal edge sharper, more knife-like; overall shape unclear. Anterolateral face of cleithrum (CLE-al, underlying posterior margin of opercle in life) smooth, subcrescentric. Basal remnant of dorsal limb of cleithrum (CLE-ld), with oblique

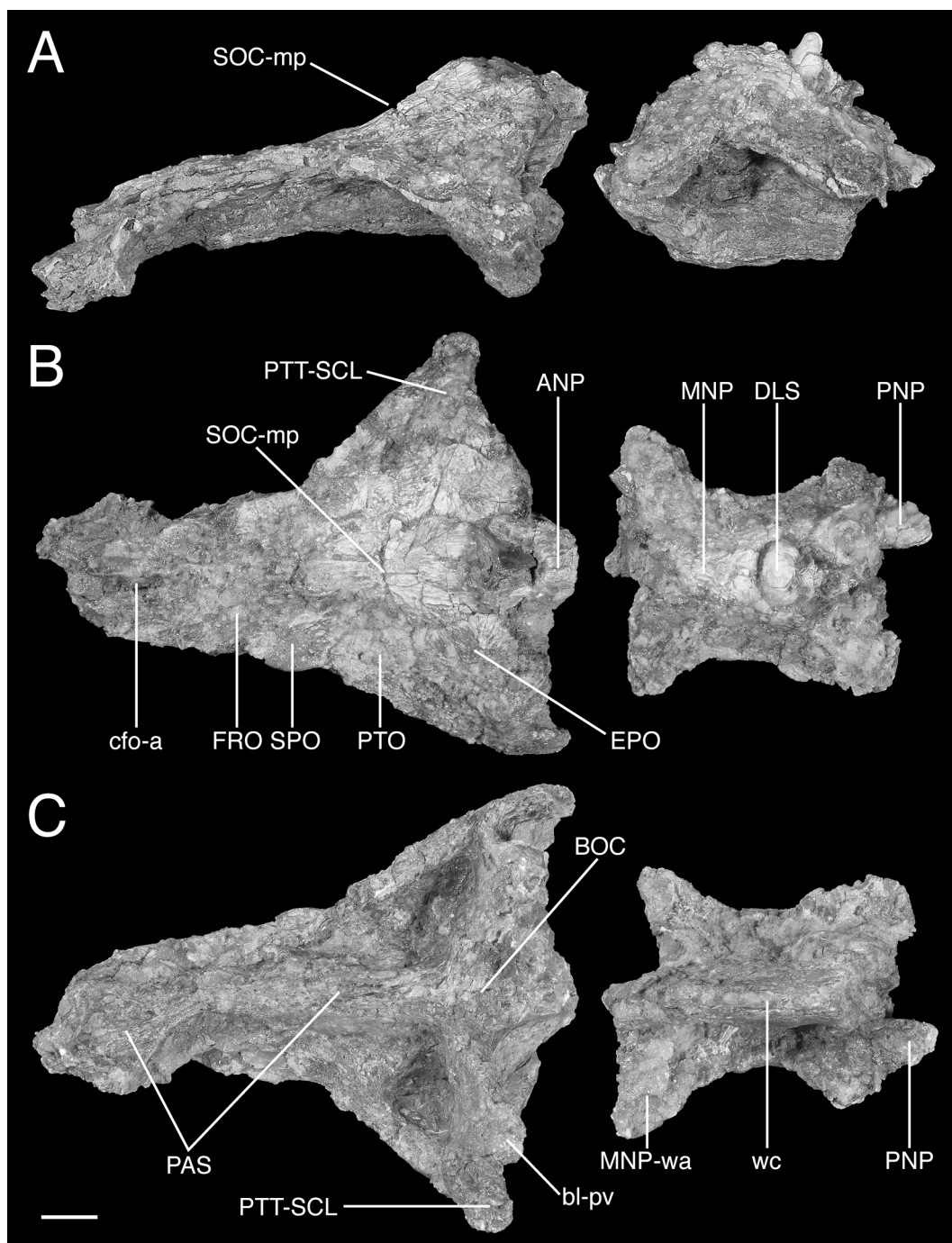


Fig. 10. Neurocranium and nuchal shield of fossil *Rhinodoras cf. thomersoni*, UNEFM-PF-0157, Urumaco Formation (middle member), Las Huertas, Venezuela. A. Lateral view (right), B. Dorsal view, C. Ventral view. Scale bar equals 1 cm, photographs by K. Luckenbill.

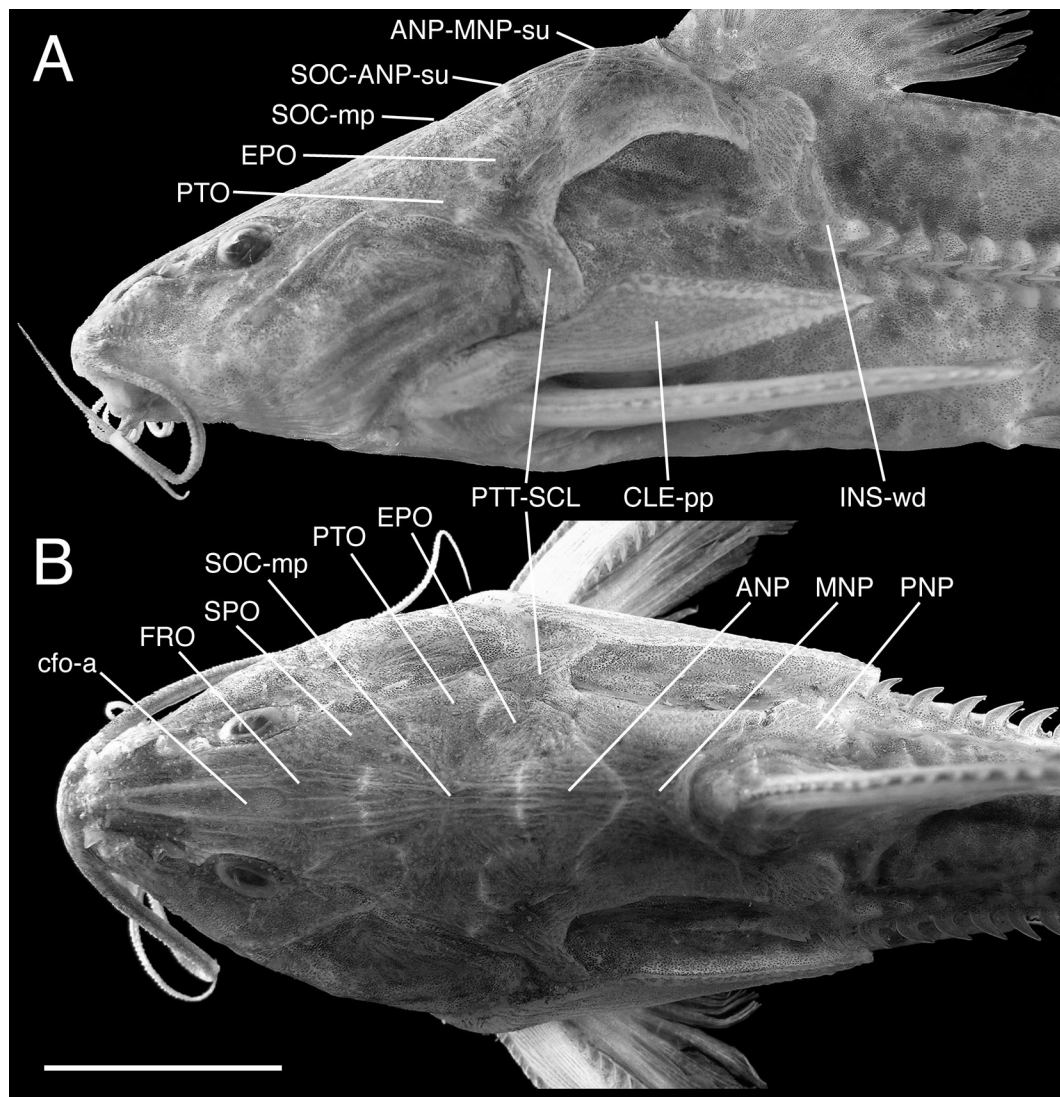


Fig. 11. Neurocranium and nuchal shield of modern *Rhinodoras thomersoni*, UF 41970, paratype (85 mm SL), Rio Catatumbo, Venezuela. A. Lateral view (left), B. Dorsal view. Scale bar equals 1 cm, photographs by M. Sabaj Pérez.

(tilted posteriorly) anterior margin and weakly concave posterior margin that finishes near vertical. Shoulder of cleithrum weakly bulging, surface ornamentation granular, lateral face transitioning relatively smoothly to that of postcleithral process.

Anterior dorsal margin of postcleithral process defined by two shallowly concave arcs that meet at about the midbase of dorsal limb of cleithrum. The more anterior arc rises from the shoulder bulge and delimits the ornamented

surface of the postcleithral process from the smooth anterolateral face of the cleithrum (CLE-al). The second arc rises to the apex of postcleithral process (coinciding with posterior base of dorsal limb of cleithrum) and is elevated by weak shelf (CLE-pp-shf) from dorsal limb of cleithrum (portion underlying posttemporal-supracleithrum in life). Proximal remnant of free dorsal margin of postcleithral process entire, straight, oblique, angled ventrally from apex and forming obtuse angle with anterior shelf (CLE-pp-shf).

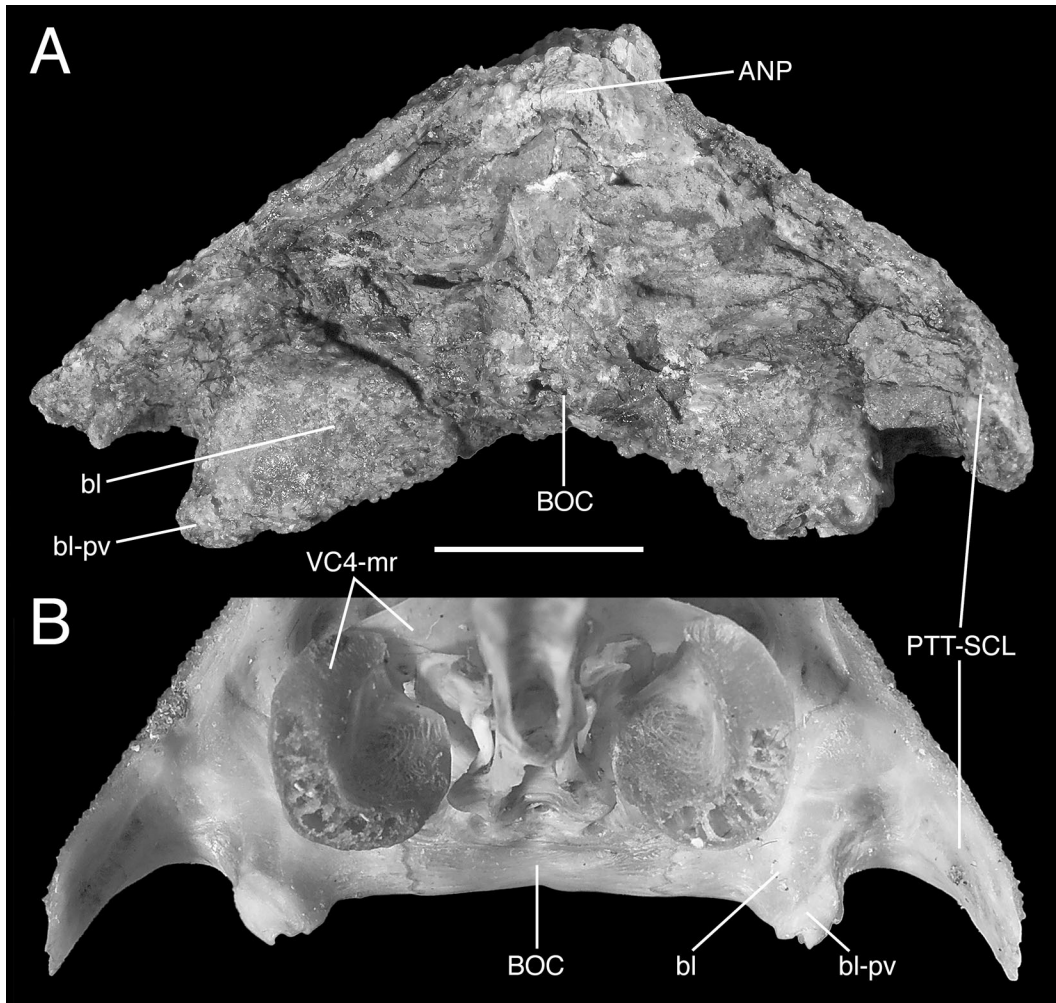


Fig. 12. Posterior view of neurocranium. A. Fossil *Rhinodoras* cf. *thomersoni*, UNEFM-PF-0157, Urumaco Formation (middle member), Las Huertas, Venezuela. B. modern *Doraops zuloagai*, ANSP 179558 (256 mm SL), Río Catatumbo, Venezuela. Scale bar equals 1 cm, photographs by K. Luckenbill.

Proximal remnant of ventral margin of postcleithral process entire, straight, weakly oblique, and partially outlining broad shallow concavity with ventral margin of shoulder bulge of cleithrum.

Lateral surface of postcleithral process with two distinct types of ornamentation (Fig. 13A; cf. Fig. 13C). Anteromedial portion with moderately fine granular surface that continues anteriorly onto shoulder bulge of cleithrum. Dorsal margin marked by band of oblique, parallel ridges and grooves; band begins below midbase of dorsal limb of cleithrum; width about 1/6 to 1/4 depth of

postcleithral process; ridges and grooves narrow, elongate, tilted posteriorly and orthogonal to proximal remnant of dorsal free margin of postcleithral process. Longitudinal carina lacking on lateral face of basal remnant of postcleithral process.

*Comparisons of neurocranium and nuchal shield.*— The fossil skull is identified as *Rhinodoras* cf. *thomersoni* based on its dorsal profile and characteristics of the nuchal shield and bones in the otic-temporal region, particularly the sphenotic. Modern *Rhinodoras* includes three nominal species, one each in the Maracaibo (*R. thomersoni*), upper

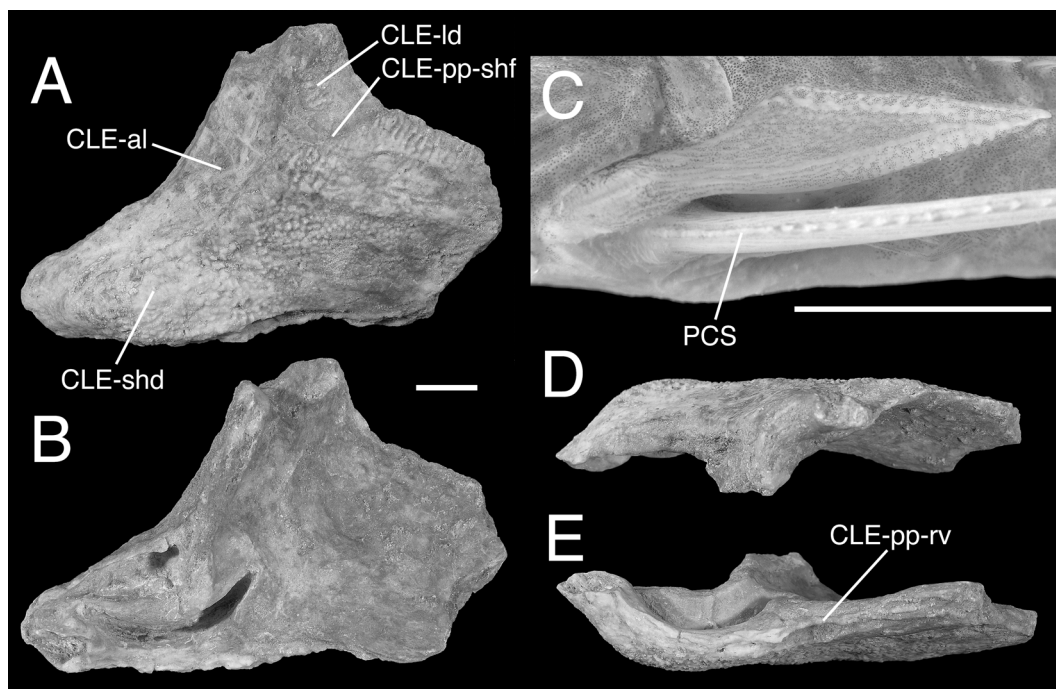


Fig. 13. Pectoral girdle of fossil (A,B,D,E) *Rhinodoras* cf. *thomersoni*, UNEFM-PF-0478, Urumaco Formation (upper member), Tío Gregorio, Venezuela, and modern (C) *R. thomersoni*, UF 41970, paratype (85 mm SL), Rio Catatumbo, Venezuela. A. Lateral view (right), B. Medial view, C. Lateral view (left), D. Dorsal view, E. Ventral view. Scale bars equal 1 cm, photographs by K. Luckenbill (A,B,D,E) and M. Sabaj Pérez (C).

to middle Amazon (*R. boehlkei*), and Paraná-Paraguay basins (*R. dorbignyi*) plus two undescribed species, one each in the Orinoco and Essequibo/upper Branco basins, respectively. In most modern *Rhinodoras* (i.e., *R. boehlkei*, *R. dorbignyi*, and the two undescribed species) the dorsal profile of the skull is moderately oblique with a shallow inflection at the supraoccipital, and levels off posteriorly, sometimes effecting the appearance of a low rounded hump spanning the distance between the middle pitline and dorsal-fin origin. In *R. thomersoni*, however, the dorsal profile is strongly oblique, and becomes gradually steeper posteriorly (particularly at middle pitline) before leveling off at about the suture between the anterior and middle nuchal plates. As a result, the dorsal profile of *R. thomersoni* has a distinct, rounded, convex hump from the middle pitline (SOC-mp) to dorsal-fin origin (Fig. 11A).

In the fossil skull the dorsal profile (Fig. 10A) is incomplete because the neurocranium and nuchal shield are broken into separate moieties across the anterior nuchal plate and epioccipitals. Nevertheless, the intact dorsal profile exhibits a distinct inflection as it begins to rise steeply just

anterior to the middle pitline of supraoccipital (SOC-mp), and is level from the suture of anterior and middle nuchal plates to posterior rim of nuchal shield. This suggests an original condition that compares most closely to modern *R. thomersoni*. Furthermore, the fossil nuchal shield (specifically, the middle nuchal plate) has deeply concave, rounded lateral margins and strongly oblique sides forming a steep triangular transverse arch. These two conditions also compare more closely to *R. thomersoni* than to other modern *Rhinodoras* wherein the nuchal shield has weakly concave lateral margins and a slightly more moderate transverse arch. It is noted that the dorsal profile of the interorbital region appears more level in the fossil than in modern *Rhinodoras*, including *R. thomersoni*.

The combination of features exhibited by the neurocranium and nuchal shield (i.e., dorsal profile with distinct inflection at supraoccipital, nuchal shield with distinct convex hump, steep triangular transverse arch and concave lateral margins) in the fossil and modern *R. thomersoni* distinguish them from most nominal doradids. These features are perhaps most closely approximated in some *Doras* and the

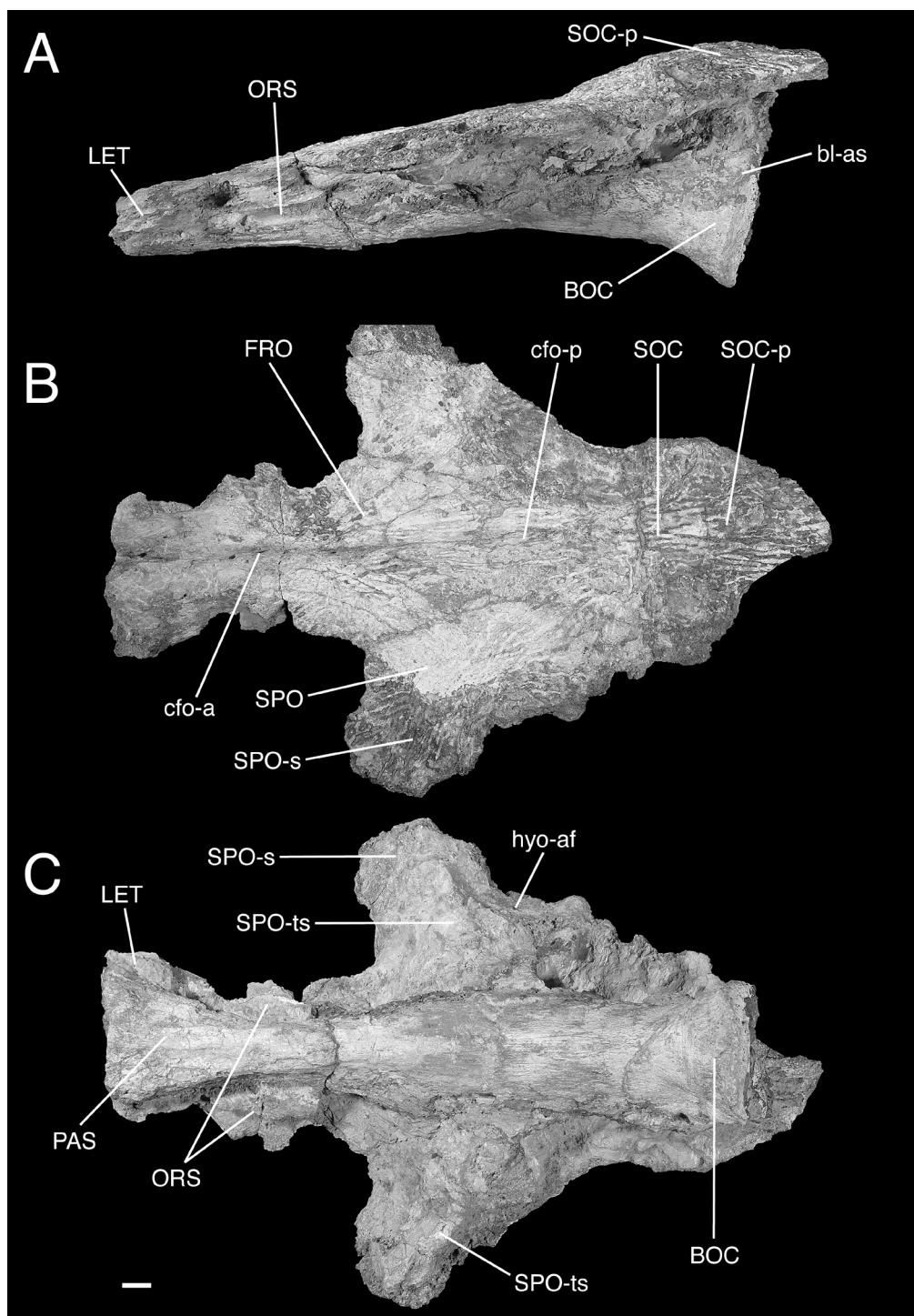


Fig. 14. Neurocranium of fossil *Platysilurus* sp., UNEFM-PF-0412, Urumaco Formation (upper member), Tío Gregorio, Venezuela. A. Lateral view (left), B. Dorsal view, C. Ventral view. Scale bar equals 1 cm, photographs by K. Luckenbill.



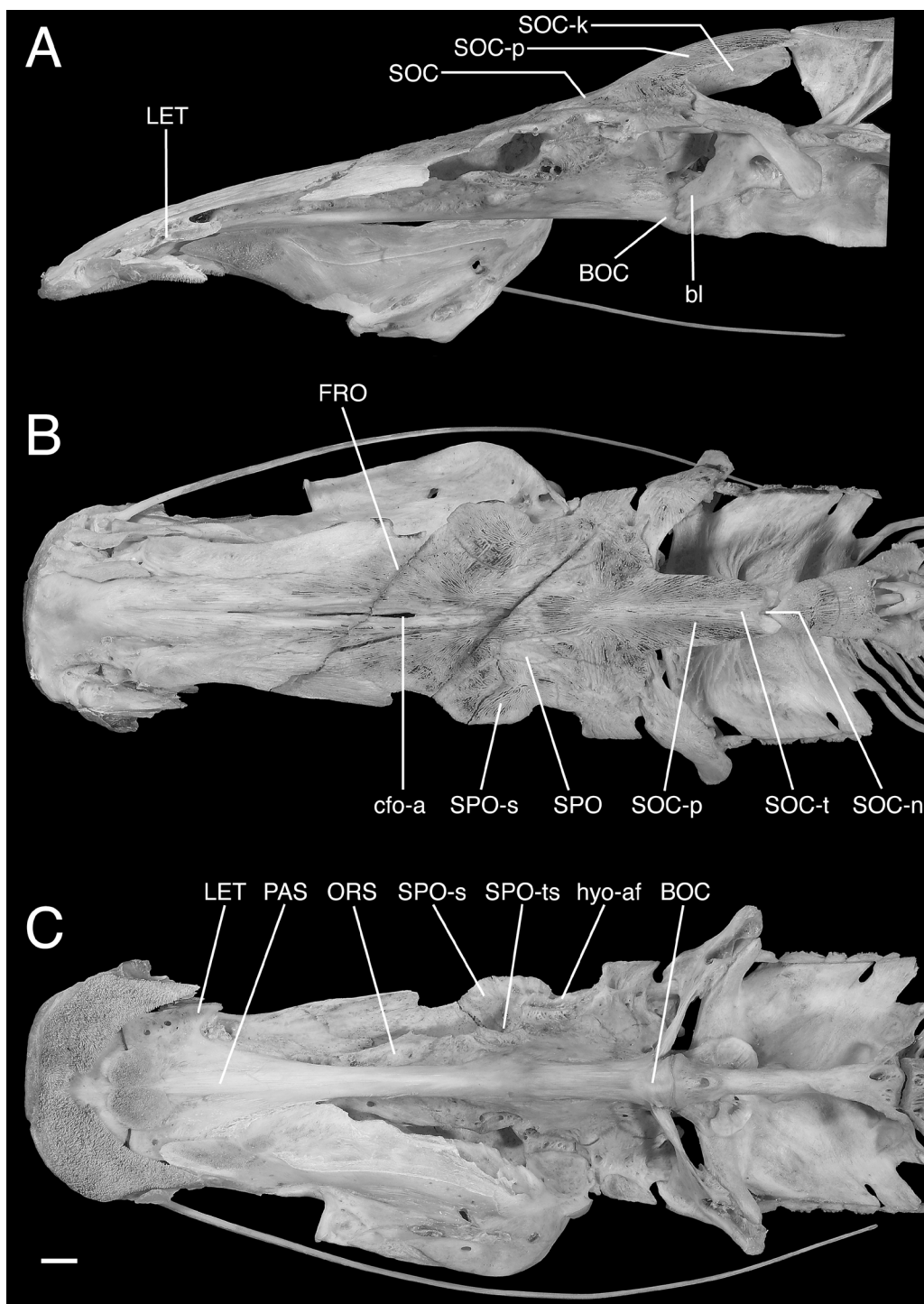


Fig. 15. Neurocranium of modern *Platytilurus malarino*, ANSP 187009 (ca. 550 mm SL), Lake Maracaibo, Venezuela. A. Lateral view (left), B. Dorsal view, C. Ventral view. Scale bar equals 1 cm, photographs by K. Luckenbill.

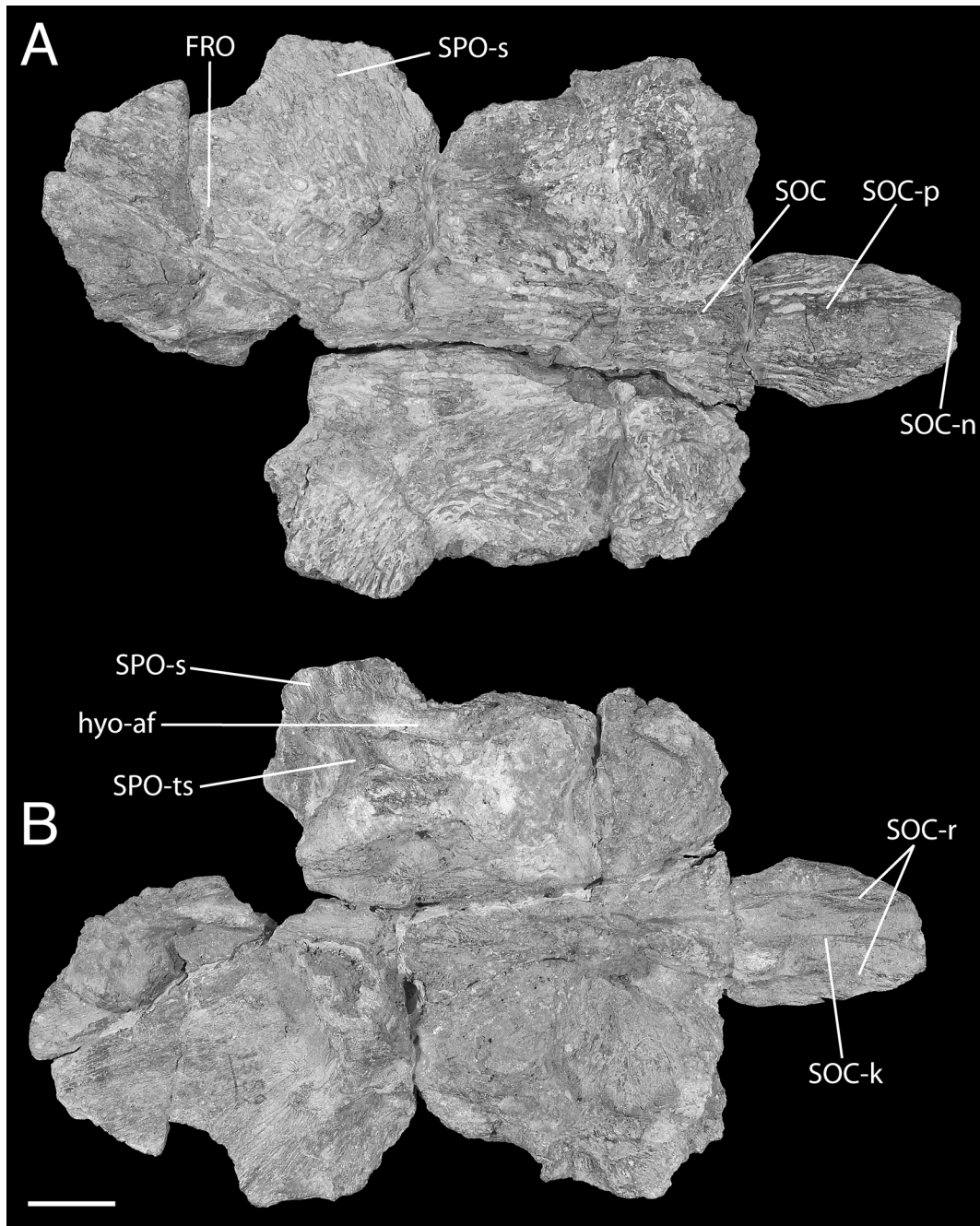


Fig. 16. Neurocranium of fossil *Platysilurus* sp., UNEFM-CIAAP-1359, Urumaco Formation (middle member), El Mamón, Venezuela. A. Dorsal view, D. Ventral view. Scale bar equals 1 cm, photographs by K. Luckenbill.

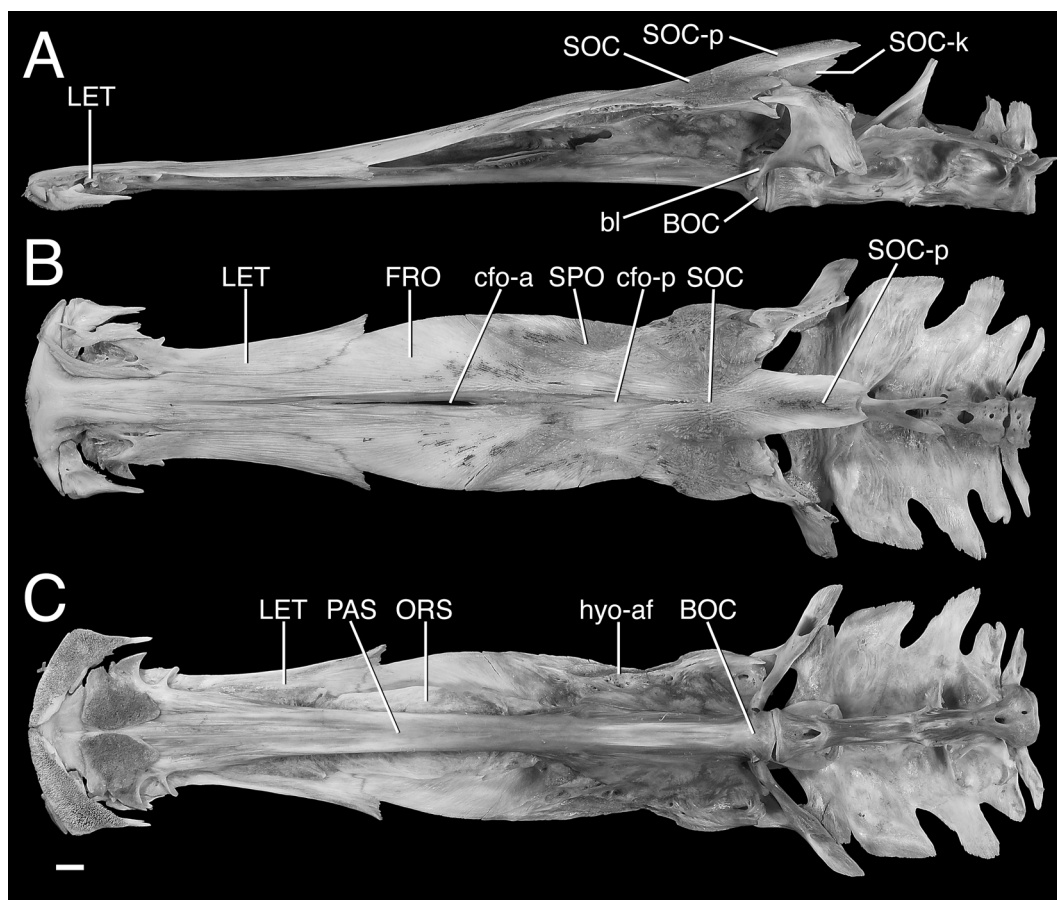


Fig. 17. Neurocranium of modern *Pseudoplatystoma tigrinum*, ANSP 187010 (ca. 810 mm SL), Rio Apure, Venezuela. A. Lateral view (left), B. Dorsal view, C. Ventral view. Scale bar equals 1 cm, photographs by K. Luckenbill.

deep-bodied species of *Trachydoras* (i.e., *T. brevis*, *T. nattereri*, *T. paraguayensis*). These taxa differ from the fossil and modern *R. thomersoni* in the specific shapes, configuration, and orientation of the bones in the otic-temporal region of the neurocranium (i.e., sphenotic, pterotic, epioccipital). Most noticeably, in the fossil and modern *R. thomersoni* the sphenotic is narrow (maximum length more than twice maximum depth), tapered to a sharp point anteriorly, and with external surface more horizontally oriented. In *Doras* and *Trachydoras* the sphenotic is deeper (maximum length about equal to or less than maximum depth), not tapered to a sharp point anteriorly, and with external surface more vertically oriented. Furthermore in *Doras* and *Trachydoras* the parasphenoid is well removed from the dorsal surface of skull (vs. moderately so in fossil).

*Comparisons of pectoral girdle.*—The fossil partial cleithrum compares most closely to that of *Rhinodoras* and *Orinocodoras* (monotypic, Orinoco basin), sister taxa (Higuchi, 1992; Birindelli, 2006) in which the postcleithral process is broad to moderately lanceolate, pointed posteriorly. Features consistent between the fossil and modern *Rhinodoras* and *Orinocodoras* are: 1) proximal free dorsal margin of postcleithral process, straight, oblique, angled ventrally from distinct apex, 2) dorsal surface of postcleithral process ornamented with distinct marginal band marked by relatively uniform pattern of parallel, oblique ridges and grooves, 3) medial and ventral surfaces of postcleithral process and lateral surface of shoulder bulge with moderately fine granular ornamentation, 4) shoulder weakly bulging and transitioning relatively smoothly to postcleithral process, and 4) overall shape of the basal portion of dorsal limb of cleithrum. Oblique grooves and ridges along the dorsal margin of the postcleithral process are sometimes observed in other non-related doradids (e.g., *Centrodoras*, *Hemidoras stenopeltis*, *Oxydoras*, *Platydoras*). *Centrodoras* differs in that 1) the dorsal margin of the postcleithral process is nearly straight, lacks a distinct apex, and is not distinctly angled ventrally beyond base of dorsal limb of cleithrum, and 2) the ornamentation on the base of the postcleithral process is striated with fine longitudinal ridges (vs. finely granular in fossil). In the other taxa the pattern of grooves and ridges is far less uniform than that of the fossil and typical of modern *Rhinodoras* and *Orinocodoras*.

The absence of a distinct longitudinal ridge or carina in the fossil distinguishes it from *Orinocodoras* and most specimens of *R. dorbignyi* (wherein the carina is variably present). Furthermore, in the fossil the apex of the dorsal margin of the postcleithral process is low, distinguishing it from *R. boehlkei* wherein the process has a tall dorsal apex that produces a relatively greater maximum depth.

It is noted that the fossil differs slightly from modern *Rhinodoras* by having anterior dorsal margin of postcleithral

process divisible into two concave arcs between its apex and the shoulder bulge compared to the single continuous concave arc observed in most specimens of modern *Rhinodoras*. Nevertheless, the fossil cleithrum compares most closely to *Rhinodoras*, and its identification as *R. cf. thomersoni* is influenced in part by the distribution of modern species of *Rhinodoras*. More comparative material, both fossil and modern, is needed to assess whether the Urumaco *Rhinodoras* is truly *R. thomersoni* or represents an undescribed species distinct from nominal *Rhinodoras*.

Family Pimelodidae  
*sensu* Lundberg and Littmann, 2003

*Platysilurus* sp.  
Figs. 14, 16

*cf. Pseudoplatystoma* sp. (in part) in Aguilera 2004:59-60  
(description, biogeography).

*cf. Pseudoplatystoma* sp. in Sánchez-Villagra and Aguilera  
2006:215 (Table 1), 217 (Fig. 2B, C).

*Material.*—Falcón State, Venezuela: UNEFM-PF-0412 (Fig. 14; cf. Fig. 15), partial neurocranium, approximately the posterior 2/3 of a skull behind a transverse break through anterior parts of parasphenoid (PAS) and frontals (FRO), lateral ethmoids (LET) and possibly posterior part of prevomer. Skull margins mostly broken but preserving proximal ends of supraoccipital posterior process (SOC-p) and laterally projecting sphenotic spines (SPO-s). 26 cm overall dorsal midline length. Locality: Urumaco Formation (upper member), Tío Gregorio. UNEFM-CIAAP-1359 (Fig. 16), partial neurocranium, approximately the posterior 2/3 of a skull roof broken on the right side through frontal and on the left through sphenotic, and lacking the braincase side walls and floor. 25.3 cm overall dorsal midline length. Locality: Urumaco Formation (middle member), El Mamón.

*Description of neurocranium.*—Skull roof (Figs. 14, 16) generally flat but supraoccipital posterior process distinctly humpbacked and frontals shallowly concave before the frontal–supraoccipital suture. Skull roofing bones sutured and coarsely ornamented with ridges and grooves trending longitudinally near midline of supraoccipital and frontals, reticulating on sphenotics (SPO). Anterior cranial fontanelle (cfo-a) narrowly open and trough-like between frontals to epiphyseal bar in a trench; posterior cranial fontanelle closed in a trench terminating posteriorly at supraoccipital. Frontal-sphenotic joint long; sphenotics large, with a prominently projecting lateral spine (SPO-s). Details of pterotic and extrascapular bones unclear.

Supraoccipital posterior process broad at base, at least as long as supraoccipital body without the process, increasingly arched in cross-section behind margin of skull roof, and its sides tapering in gently convex arcs. Terminus of supraoccipital posterior process is broken in both specimens. In UNEFM-CIAAP-1359, however, the posteriorly-directed fracture surface of the process shows the anterior end of a matrix-filled cavity (Fig. 16, SOC-n) that is either the anterior end of a dorsomedian trench or a deep notch into which the anterior nuchal plate articulated.

Ventral side of UNEFM-PF-0412 (Fig. 14C) dominated by heavy midventral parasphenoid (PAS) stem, basioccipital (BOC), and laterally projecting sphenotic spines. Parasphenoid stem broadly flaring anteriorly below orbitosphenoid, narrowest below posterior end of orbitosphenoid (ORS), and broadening posteriorly as braincase floor and sidewalls, posteriorly suturing deeply with basioccipital. Parasphenoid joints with pterosphenoids, sphenotics, prootics and exoccipitals indistinctly preserved. Orbitosphenoid in broad contact with frontals (FRO) dorsally and parasphenoid ventrally, its sidewalls relatively deep, nowhere very depressed, and bearing prominent horizontal shelves. Orbitosphenoid shelves twice as broad as narrowest width of parasphenoid and anteriorly converging with skull roof and parasphenoid stem onto posterior side of lateral ethmoid (LET). Details of pterosphenoids unclear; sidewalls of prootics broken. In both specimens, ventral sides of sphenotics show sharply elevated transverse struts (SPO-ts) extending laterally below sphenotic spines. Hyomandibular facet best preserved on UNEFM-CIAAP-1359 (hyo-af) as a shallow, laterally-concave and elongate trench beginning on posterior side of sphenotic spine, terminating on anterior end of pterotic, about 70% of facet formed by sphenotic and 30% by pterotic. Basioccipital much expanded to form deeply ovoid and flat-faced occipital condyle; laterally bearing coarse attachment surface of the ossified transcapular (Baudelot's) ligament. Exoccipitals evident only as distorted fragments; details of epioccipitals unclear. Ventral side of supraoccipital posterior process bearing a strong median keel (SOC-k) and a pair of symmetrically diverging low ridges (SOC-r).

*Comparisons of neurocranium.*—Identification of these fossils as *Platysilurus* is based on general similarity of skull roof and basicranial shape, dermal bone ornamentation pattern, and arrangement of bony elements compared to the two modern species: *P. malarma* (Maracaibo basin) and *P. mucosus* (Orinoco, Amazon, large rivers of the Guianas). Specifically, fossil and modern *Platysilurus* differ from other pimelodids in their possession of the following character combination (Figs. 14, 15, 16): arched to humpbacked and broad supraoccipital process underlain by both a median keel and paired parasagittal ridges, cranial fontanelle not

entering supraoccipital, prominent sphenotic spine underlain by a thickened transverse strut, and relatively deep orbitosphenoid.

The fossil catfish differs from modern *Platysilurus malarma* and *P. mucosus* in its wider angle of anterior expansion of the parasphenoid (Fig. 14C; cf. Fig. 15C) and the anterior projection of orbitosphenoid shelves to the lateral ethmoid (Figs. 14A, C; cf. Figs. 15A, C). Both of these features suggest a broader, more foreshortened snout in the fossil, but lacking more complete preservation of the anterior head skeleton this needs confirmation by additional specimens. The fossil also differs from modern *Platysilurus* in having a more deeply expanded basioccipital condyle (Figs. 14A, C; cf. Figs. 15A, C) and lacking a long dorsomedian trench on the supraoccipital process (Fig. 14B; cf. Fig. 15B, SOC-t). In large compared to small specimens of *P. malarma*, however, the dorsomedian trench is reduced in depth and length suggesting that its apparent absence in the larger fossil skulls could be due to their great size. As indicated above in UNEFM-CIAAP-1359 (Fig. 16) the broken end of the supraoccipital process shows either the anterior end of a dorsomedian trench or the deep notch-like joint (SOC-n) with the anterior nuchal plate.

Among other pimelodids the fossil *Platysilurus* most resembles *Pseudoplatystoma* (Fig. 17). *Pseudoplatystoma*, however, differs strongly in having a much more depressed skull anteriorly, less prominently bulging supraoccipital process, obsolete sphenotic spine, sphenotic without raised transverse struts ventrally, and more elongate cranial fontanelle reaching onto the supraoccipital. Other pimelodid genera are even more distinct from the fossil and *Platysilurus*.

## DISCUSSION

*Doras dioneae* represents the first fossil doradid to be formally described as a new species. The other Urumaco fossils described here are the first to be identified for their representative genera: *Doraops* and *Rhinodoras* (Doradidae) and *Platysilurus* (Pimelodidae). A fifth freshwater catfish from the Urumaco formation is the recently described pimelodid *Phractocephalus nassi* (Lundberg and Aguilera, 2003). Other fossil catfishes from Miocene-lower Pliocene deposits in the Urumaco area belong to the primarily marine family Ariidae and include eight essentially modern species common to estuarine environments along the Atlantic and Pacific coasts of southern Central and northern South America (Aguilera and Aguilera, 2004).

The freshwater fossil catfishes described herein, or their close ancestors, inhabited the "Paleo-Amazon-Orinoco", a large and long-persistent river system that originated far south in western Amazonia, flowed north in the Andean

foreland basin to empty into the Caribbean on the north coast of South America (Hoorn, 1993, 1994a, b, c; Hoorn et al., 1995; Lundberg et al., 1998). The outlet of this ancient river system supported a rich diversity of large aquatic vertebrates that characterize a complex mixture of continental (savannas), freshwater (swamps and rivers), estuarine (brackish) and marine (coastal lagoon, salt marsh and sandy littoral) paleo-environments (Lundberg and Aguilera, 2003; Aguilera, 2004; Sánchez-Villagra and Aguilera, 2006). Sometime in the Late Miocene (ca. 8 Ma), the rising mountain divides of the Eastern Andes and Coastal Cordilleras isolated the Caribbean outlet of the “Paleo-Amazon-Orinoco” and established the modern west-to-east Atlantic drainages of the Amazon and Orinoco river systems (Lundberg et al., 1998). This had a profound biotic effect resulting in numerous extinctions among the resident fauna (Lundberg and Aguilera, 2003; Aguilera, 2004; Sánchez-Villagra and Aguilera, 2006)

The “Paleo-Amazon-Orinoco” river system is fragmented in today’s fluvial landscape into the Maracaibo Basin which represents its lowermost course and outlet (in part), the Orinoco which receives waters formerly associated with its middle course, and the Amazon and possibly the extreme northern headwaters of the Paraná-Paraguay system which now drain the upper portion of this ancient watershed. The Urumaco fossil freshwater catfishes together with present-day distributions of related taxa document four separate fates for the Late Miocene fauna of the “Paleo-Amazon-Orinoco”.

The first, supported by fossil doradids *Doraops* cf. *zuloagai* and *Rhinodoras* cf. *thomersoni*, is the persistence of related lineages in the present-day trans-Andean (Maracaibo), and cis-Andean (Orinoco, Amazon, Paraná-Paraguay) basins. Modern *Doraops zuloagai* is endemic to the Maracaibo Basin where it occurs in medium-sized freshwater rivers and along the southern littoral of Lake Maracaibo. Cladistic analyses of molecular (Moyer et al., 2004) and morphological (Birindelli, 2006) data place *Doraops* sister to *Pterodoras*, a freshwater channel dweller that is widespread in medium to large rivers in the Orinoco, Amazon, and Paraná-Paraguay basins. The fossil *Doraops* establishes the minimum age of divergence of *Doraops* and *Pterodoras* at about 8 Ma. Modern *Rhinodoras* persists in the Maracaibo (*R. thomersoni*), Orinoco (one undescribed species), Amazon (*R. boehlkei* and one undescribed species) and Paraná-Paraguay (*R. dorbignyi*) basins where it inhabits freshwaters of small to large rivers. The cis-Andean *R. boehlkei* and *R. dorbignyi* form a sister group related to *R. thomersoni* and this clade is sister to the monotypic Orinoco endemic *Orinocodoras eigenmanni* (Birindelli, 2006). If the undescribed *Rhinodoras* are more closely related to the cis-Andean species, the minimum age of divergence of *R. thomersoni* from the other *Rhinodoras* is simi-

larly set at about about 8 Ma.

The second scenario, supported by fossil pimelodid *Platysilurus*, is the persistence of “Paleo-Amazon-Orinoco” lineages in the Maracaibo, Orinoco and Amazon. Modern *Platysilurus* occur in freshwater in the Maracaibo basin (*P. malarma*) and widely throughout the Orinoco and Amazon basins (*P. mucosa*). The modern species of *Platysilurus* are considered to be a vicariant sister-species pair whose common ancestor lived before dismemberment of the paleo-Amazon-Orinoco. The fossil Urumaco *Platysilurus* is similar in its large size to *P. malarma* but differs from both modern species in the form of the parasphenoid stem and anterior extent of the orbitosphenoid shelves. Without more complete anatomical information on the Urumaco *Platysilurus* we cannot speculate on its possible relationships to the modern species. Nevertheless the minimum age for the origin of this genus is about 8 Ma.

The third scenario, supported by fossil pimelodid *Phractocephalus nassi*, involves persistence in the Orinoco and Amazon, but extinction in the Maracaibo (Lundberg et al., 1988; Lundberg and Aguilera, 2003). The single modern species, *P. hemioliopterus*, ranges widely in medium to large freshwater rivers throughout the lowland Orinoco and Amazon basins and at least two large coastal drainages of the Guianas (i.e., Corantijn and Essequibo; Ouboter and Mol, 1993; Lundberg and Aguilera, 2003)

The fourth scenario, supported by fossil species *Doras dioneae*, involves persistence in the Amazon basin, but extinction in the Maracaibo and presumably Orinoco. Modern *Doras* is restricted to freshwater in the middle to lower Amazon basin (three undescribed species) and coastal drainages of the Guianas (*D. carinatus* and *D. micropoetus*) where it occurs primarily in medium to large rivers in lowland areas (elevation <200 m). *Doras* is not known to occur in the present-day Orinoco basin.

The Urumaco freshwater fossil catfishes and persistence of related modern taxa in the Maracaibo, Orinoco, Amazon and Paraná-Paraguay basins corroborates historical links among these basins via the “Paleo-Amazon-Orinoco” river system. The extinctions of *Phractocephalus nassi* and *Doras dioneae* in the Maracaibo basin were concomitant or subsequent to the isolation of the lowermost portion of the “Paleo-Amazon-Orinoco” to the coastal region of northwestern Venezuela about 8 Ma. The absence of *Doras* from the modern Orinoco is somewhat puzzling in that it suggests a second extinction event not evident for the other catfishes.

## ACKNOWLEDGEMENTS

The Academy of Natural Sciences of Philadelphia and the Universidad Nacional Experimental Francisco de Miranda encouraged this collaborative work. We thank K.R. Luckenbill (ANSP) for preparing the figures. For loans of specimens and help and hospitality during museum visits we thank: J. Armbruster, N. Lujan, D. Werneke (AUM), J.D. Bogotá, J.A. Maldonado (IAvH), M. Arce (ICNMHN), C. Mayer (INHS), A. Akama, A.L. Canto, L. Rapp Py-Daniel, L.M. Sousa (INPA), F. Provenzano, H. Lopez-Rojas (MBUCV), R.E. Reis (MCP), R. Covain, S. Fisch-Muller (MHNG), M. Azpelicueta (MLP), P. Pruvost (MNHN), J.L. Birindelli, O.T. Oyakawa (MZUSP), and R. Robins (UF). The U.S. National Science Foundation supported this work through research grants to the All Catfish Species Inventory (NSF DEB-0315963) and J. G. Lundberg (DEB-0089612).

## LITERATURE CITED

- Aguilera S., O. A. 2004. Tesoros paleontológicos de Venezuela: Urumaco, patrimonio natural de la humanidad. Universidad Nacional Experimental Francisco de Miranda, Santa Ana de Coro, Venezuela. 148 p.
- Aguilera, O., and D. Rodrigues de Aguilera. 2004. Amphi-American Neogene sea catfishes (Siluriformes, Ariidae) from northern South America, p. 29–48. *In*: M. R. Sánchez-Villagra and J. A. Clack (eds.), *Fossils from the Miocene Castillo Formation, Venezuela: contributions in Neotropical Palaeontology. Special Papers in Palaeontology*, 71.
- Arratia, G., and A. Cione. 1996. The record of fossil fishes of southern South America, p. 9–72. *In*: G. Arratia (ed.), *Contributions of southern South America to vertebrate paleontology*, *Münchener Geowiss. Abh. (A)* 30, F. Pfeil, München.
- Berg, L. S. 1940. Classification of fishes, both recent and fossil. *Travaux de l'Institut Zoologique de l'Academie des Sciences de l'URSS*, 5: 87–517 (English translation, Ann Arbor, Michigan, 1947).
- Birindelli, J. L. O. 2006. Revisão taxonômica e filogenia do gênero *Rhinodoras* Bleeker, 1862 (Siluriformes, Doradidae). Unpublished M.S. dissertation, Universidade de São Paulo, Instituto de Biociências, 274 p.
- Cione, A. L. 1978. Aportes paleontológicos al conocimiento de la evolución de las paleotemperaturas en el área austral de América del Sur durante el Cenozoico. *Ameghiniana*, 15(1-2): 183–208.
- Cione, A. L. 1986. Los peces continentales del Cenozoico de Argentina: Su significación paleoambiental y paleobiogeográfica, p. 101–106. *In*: *Evolución de los Vertebrados Cenozoicos de América del Sur [simposio]*, Actas IV Congreso Argentino de Paleontología y Bioestratigrafía, 2.
- Díaz de Gamero, M. L. 1996. The changing course of the Orinoco River during the Neogene: a review. *Palaeogeography, Palaeoclimatology and Palaeoecology*, 123: 385–402.
- Díaz de Gamero, M. L., and O. J. Linares. 1989. Estratigrafía y paleontología de la Formación Urumaco, del Mioceno Tardío de Falcón Noroccidental. VII Congreso Geológico Venezolano, *Memorias*, 1: 419–438.
- Eigenmann, C. H. 1912. The freshwater fishes of British Guiana, including a study of the ecological grouping of species, and the relation of the fauna of the plateau to that of the lowlands. *Memories of the Carnegie Museum*, 5(1): i–xxii + 1–578, Pls. 1–103.
- Flynn, J. J., J. Guerrero and C. C. Swisher III. 1997. Geochronology of the Honda Group, p. 44–59. *In*: R. F. Kay, R. H. Madden, R. L. Cifelli and J. J. Flynn (Eds.), *Vertebrate paleontology in the Neotropics: The Miocene fauna of La Venta, Colombia*. Smithsonian Institution Press, Washington, 592 p.
- Hambalek, N., V. Rull, E. Digiacomo and M. L. Díaz de Gamero. 1994. Evolución paleoecológica y paleoambiental de la secuencia del Neógeno en el surco de Urumaco, estado Falcón. *Estudio palinológico y litológico*. *Boletín de la Sociedad Venezolana de Geología*, 19(1–2): 7–19.
- Horn, C. 1993. Marine incursions and the influence of Andean tectonics on the Miocene depositional history of northwestern Amazonia: results of a palynostratigraphic study. *Palaeogeography, Palaeoclimatology and Palaeoecology*, 105: 267–309.
- Horn, C. 1994a. Miocene palynostratigraphy and paleoenvironments of northwestern Amazonia: evidence for marine incursions and the influence of Andean tectonics. Unpublished Ph.D. dissertation, Free University of Amsterdam, The Netherlands, 156 p.
- Horn, C. 1994b. Fluvial palaeoenvironments in the intracratonic Amazon Basin (Early Miocene to early Middle Miocene, Colombia). *Palaeogeography, Palaeoclimatology and Palaeoecology*, 109: 1–55.
- Horn, C. 1994c. An environmental reconstruction of the palaeo-Amazon River system (middle-late Miocene, NW Amazonia). *Palaeogeography, Palaeoclimatology and Palaeoecology*, 112: 187–238.
- Horn, C., J. Guerrero, G. A. Sarmiento and M. A. Lorente. 1995. Andean tectonics as a cause for changing drainage patterns in Miocene northern South America. *Geology*, 23: 237–240.
- Higuchi, H. 1992. A phylogeny of the South America thorny catfishes (Osteichthyes; Siluriformes, Doradidae). Unpublished Ph.D. dissertation, Harvard University, Cambridge, Massachusetts, 372 p.
- Lacépède, B. G. E. 1803. *Histoire naturelle des poissons*, 5: i–lxviii + 1–803 + index, Pls. 1–21.
- Leviton, A. E., R. H. Gibbs, Jr., E. Heal and C. E. Dawson. 1985. Standards in herpetology and ichthyology: Part I. Standard symbolic codes for institutional resource collections in herpetology and ichthyology. *Copeia* 1985(3): 802–832.
- Linnaeus, C. 1766. *Systema naturae sive regna tria naturae, secundum classes, ordines, genera, species, cum characteribus, differentiis, synonymis, locis*, 12<sup>th</sup> ed. Laurentii Salvii, Holmiae, 1(1): 1–532.
- Lundberg, J. G. 1997. Freshwater fishes and their paleobiotic implications, p. 67–91. *In*: R. F. Kay, R. H. Madden, R. L. Cifelli and J. J. Flynn (Eds.), *Vertebrate paleontology in the Neotropics: The Miocene fauna of La Venta, Colombia*. Smithsonian Institution Press, Washington, 592 p.

- Lundberg, J. G. 1998. The temporal context for the diversification of Neotropical fishes, p. 49–68. *In*: L. R. Malabarba, R. E. Reis, R. P. Vari, Z. M. S. Lucena and C. A. S. Lucena (Eds.), Phylogeny and classification of Neotropical fishes. EDIPUCRS, Porto Alegre, Brazil, 603 p.
- Lundberg, J. G. 2005. *Brachyplatystoma promagdalenae* n. sp., a fossil goliath catfish (Siluriformes: Pimelodidae) from the Miocene of Colombia, South America. *Neotropical Ichthyology*, 3(4): 597–605.
- Lundberg, J. G., and O. A. Aguilera. 2003. The late Miocene *Phractocephalus* catfish (Siluriformes: Pimelodidae) from Urumaco, Venezuela: additional specimens and reinterpretation as a distinct species. *Neotropical Ichthyology*, 1(2): 97–109.
- Lundberg, J. G., O. J. Linares, M. E. Antonio and P. Nass. 1988. *Phractocephalus hemiliopterus* (Pimelodidae, Siluriformes) from the Upper Miocene Urumaco Formation, Venezuela: a further case of evolutionary stasis and local extinction among South American fishes. *Journal of Vertebrate Paleontology*, 8(2): 131–138.
- Lundberg, J. G., L. G. Marshall, B. H. Guerrero, M. C. Malabarba and F. Wesselingh. 1998. The stage for Neotropical fish diversification: a history of tropical South American rivers, p. 13–48. *In*: L. R. Malabarba, R. E. Reis, R. P. Vari, Z. M. S. Lucena, and C. A. S. Lucena (Eds.), Phylogeny and classification of Neotropical fishes. EDIPUCRS, Porto Alegre, Brazil, 603 p.
- Lundberg, J. G., and M. W. Littmann. 2003. Family Pimelodidae (Long-whiskered catfishes). p. 432–446. *In*: R. E. Reis, S. O. Kullander, and C. J. Ferraris (eds.), Check list of freshwater fishes of South and Central Americas, EDIPUCRS, Porto Alegre, Brazil, 603 p.
- Marshall, L. G., and T. Sempere. 1993. Evolution of the Neotropical Cenozoic Land Mammal Fauna in its geochronologic, stratigraphic, and tectonic context. p. 329–392. *In*: P. Goldblatt (ed.), Biological Relationships between Africa and South America, Yale University Press, New Haven, 630 p.
- Ministerio De Energía y Minas. 1997. *Léxico Estratigráfico de Venezuela* (Tercera Edición). Boletín de Geología, 12, 828 pp.
- Moyer, G. R., B. M. Burr and C. Krajewski. 2004. Phylogenetic relationships of thorny catfishes (Siluriformes: Doradidae) inferred from molecular and morphological data. *Zoological Journal of the Linnean Society* 140: 551–575.
- Ouboter, P. E., and J. H. A. Mol. 1993. The fish fauna of Suriname, p. 133–154. *In*: P. E. Ouboter (ed.), Freshwater ecosystems of Suriname. Kluwer Academic Publishers, Dordrecht, The Netherlands, 313 p.
- de Pinna, M. C. C. 1998. Phylogenetic relationships of Neotropical Siluriformes (Teleostei: Ostariophysi): historical overview and synthesis of hypotheses, p. 279–330. *In*: L. R. Malabarba, R. E. Reis, R. P. Vari, Z. M. S. Lucena, and C. A. S. Lucena (eds.). Phylogeny and Classification of Neotropical fishes. EDIPUCRS, Porto Alegre, Brazil, 603 p.
- Sabaj, M. H. 2005. Taxonomic assessment of *Leptodoras* (Siluriformes: Doradidae) with descriptions of three new species. *Neotropical Ichthyology*, 3: 637–678.
- Sabaj, M. H., and C. J. Ferraris, Jr. 2003. Family Doradidae (Thorny catfishes). p. 456–469. *In*: R. E. Reis, S. O. Kullander, and C. J. Ferraris (eds.), Check list of freshwater fishes of South and Central Americas, EDIPUCRS, Porto Alegre, Brazil, 603 p.
- Sánchez-Villagra, M. R., O. A. Aguilera, and I. Horowitz. 2003. The anatomy of the world's largest rodent. *Science*, 301(5640):1678–1679.
- Sánchez-Villagra, M. R. and O. A. Aguilera. 2006. Neogene vertebrates from Urumaco, Falcón State, Venezuela: diversity and significance. *Journal of Systematic Palaeontology*, 4(3): 213–220.
- Schultz, L. P. 1944. The catfishes of Venezuela, with descriptions of thirty-eight new forms. *Proceedings of the United States National Museum*, 94(3172): 173–338, Pls. 1–14.
- Taphorn, D. C., and C. G. Lilyestrom. 1984. *Rhinodoras thomersoni*: un bagre sierra nuevo en Venezuela (Pisces, Doradidae). *Revista UNELLEZ de Ciencia y Tecnología*, 2(2): 87–92.

### Appendix 1

#### Comparative doradids examined

*Acanthodoras cataphractus*.—**Guyana**: ANSP 175877 (2 alc), clearwater creek (Essequibo Dr.), ca. 5.3 km from Kurupukari field station (04°38'00"N, 058°42'59"W), W.G. Saul, et al., 5 Feb 1997, WGS97-37. *Acanthodoras spinosissimus*.—**Guyana**: ANSP 179421 (2 alc, 1 skel), Simoni River (Rupununi Dr.), 4 stations along river from 6.6 km SE to 3.2 km W of Karanambo Ranch (03°43'09"N, 059°15'40"W), M.H. Sabaj, et al., 29 Oct 2002, GUY 02-11. *Agamyxis pectinifrons*.—**Peru**: Loreto: INHS 43281 (2 alc), Rio Itaya and Quebrada Mazana (Amazonas Dr.), south of Iquitos (03°49'48"S, 73°18'03"W), M.H. Sabaj, et al., 28 Jul 1997, Peru 97-7. *Amblyodoras affinis*.—**Peru**: Loreto: ANSP 139291 (21 alc), Rio Nanay (Amazonas Dr.), opposite naval base, ca. 6.8 km above Rio Amazonas, C.C.G. Chaplin, et al., 12 Oct 1955, P55-12. *Anadoras grypus*.—**Peru**: Loreto: ANSP 166262 (3 alc), trib. Rio Yanayacu (Amazonas Dr.), W of Miraflores (04°42'S, 074°17'W), P. Fromm, et al., 21 Aug 1989, PF89-5; ANSP 179473 (1 skel), Moena Cano and mouth of Ullpa Cano, a trib. of Moena Cano (R. Itaya-Amazonas Dr.), just southeast of Belen, Iquitos (03°46'19"S, 073°14'16"W), M.H. Sabaj, et al., 15 Aug 2003, PERU 2003-03. *Anduzedoras oxyrhynchus*.—**Brazil**: Amazonas: ANSP 178551 (1 skel), Rio Negro, between Vila Guajara (upstream) and Carvoeiro (downstream), upstream from confluence with Rio Jufari (01°12'34"S, 062°13'47"W), J.G. Lundberg, et al., 10 Dec 1993, JGL-93-193; **Venezuela**: Amazonas: ANSP 180293 (2 alc, 1 skel), Rio Ventuari (Orinoco Dr.), beach at village of Moriche, 116 km NE of Macuruco, 169 km NE of San Fernando de Atabapo (04°45'N, 066°21'13"W), M.H. Sabaj, et al., 7 Apr 2004, VEN 04-15. *Astrodoras asterifrons*.—**Brazil**: Amazonas: ANSP 179556 (1 skel), Rio Negro (Amazonas Dr.), 10.2 km downriver of Santa Maria, 19.4 km upriver of Leprosario (03°01'18"S, 060°24'55"W), J.G. Lundberg, et al., 13 Dec 1993, JGL-93-209; Para: ANSP 177996 (1 alc), Rio Trombetas (Amazonas Dr.), 4.6 km downriver of Santa Cecilia, 21.4 km upriver of Oriximina (01°38'52"S, 055°57'35"W), R.E. Reis, et al., 26 Oct 1994, RER-94-020; ANSP 181034 (2 alc), Rio Acarai (Xingu-Amazonas Dr.), 42 km upriver



of Porto de Moz (02°03'11"S, 052°18'09"W), A.M. Zanata, et al., 10 Nov 1994, AMZ-94-068. *Centrochir crocodili*.—**Colombia**: Santander: CU 47930 (1 alc), Lake San Sylvestre (Magdalena Dr.), near city of Barranca-Bermeja, F. Archer and J.D. Archer, 20 Aug 1964. *Centrodoras brachiatus*.—**Brazil**: Amazonas: ANSP 178542 (1 alc), Rio Solimoes (Amazonas Dr.), 5.6 km upstream from Pananim, 11.1 km downstream from Alvaraes (03°15'55"S, 064°43'44"W), O.T. Oyakawa, et al., 30 Oct 1993, OTO-93-009; ANSP 179155 (1 skel, 258 mm), Rio Solimoes (Amazonas Dr.) above R. Jutai, 24.4 km downstream of Petrolina, 10 km upstream of Siria (02°44'15"S, 066°56'07"W), J.G. Lundberg, et al., 17 Nov 1993, JGL-93-072; ANSP 179164 (1 skel, 217 mm SL), Rio Solimoes (Amazonas Dr.), near Sao Antonio do Ica, J.G. Lundberg, et al., 1993, JGL-93-000A; ANSP 179165 (2 skel), Rio Amazonas (Atlantic O. Dr.), above mouth of Rio Madeira (03°18'31"S, 058°46'23"W), M.W. Westneat, et al., 13 Oct 1994, MWW-94-026; ANSP 179175 (1 skel, 103 mm SL), Rio Solimoes (Amazonas Dr.), near Tefe, J.G. Lundberg, et al., 1993, JGL-93-000C; ANSP 179243 (1 skel), Rio Solimoes (Amazonas Dr.), near Parana do Mamia, 24 km downriver of Vila Paricatuba, 22.5 km upriver of Nazario (03°54'16"S, 062°46'00"W), J.P. Sullivan, et al., 27 Oct 1993, JPS-93-005; ANSP 185163 (1 alc, 259 mm), Rio Solimoes (Amazonas Dr.), 25 km downriver of Vila Iranduba, 14 km upriver of Vila Careiro (03°16'17"S, 059°55'50"W), C. Cox-Fernandes, et al., 21 Jul 1996, CCF-96-039; Para: ANSP 179245 (1 skel, 218 mm), Rio Amazonas (Atlantic Dr.) below R. Trombetas, 31.4 km downriver of Obidos, 84.3 km upriver of Santarem (02°07'51"S, 055°16'08"W), J.G. Lundberg, et al., 28 Oct 1994, JGL-94-083. *Centrodoras hasemani*.—**Brazil**: Amazonas: ANSP 177907 (1 alc, 210 mm), Rio Negro (Amazonas Dr.), near mouth of Rio Branco, W of Moura (ca. 01°30'S, 061°48'W), J. Faughn, et al., Apr-Jun 1967; ANSP 179555 (2 skel, 105.1-108.4 mm), Rio Negro (Amazonas Dr.), 10.2 km downriver of Santa Maria, 19.4 km upriver of Leprosario (03°01'18"S, 060°24'55"W), J.G. Lundberg, et al., 13 Dec 1993, JGL-93-209; ANSP 181036 (1 alc), Rio Negro (Amazonas Dr.), 40 km upriver of S.,o Francisco de Assis (01°44'55"S, 061°25'00"W), J.P. Friel, et al., 11 Dec 1993, JPF-93-184; Venezuela: Amazonas: ANSP 182227 (1 alc, 210 mm), Rio Casiquiare (Negro Dr.), bedrock outcrop 59.5 km SW of La Esmerelda (02°49'07"N, 065°57'19"W), M.H. Sabaj, et al., 8 Mar 2005, VEN 05-18. *Centrodoras* sp.—**Brazil**: Amazonas: ANSP 179172 (1 skel, 220 mm SL), Rio Negro (Amazonas Dr.) 8.6 km downstream of Punta Negra, 9 km upstream of Manaus (03°07'49"S, 060°05'07"W), J.G. Lundberg, et al., 21 Oct 1993, JGL-93-003; INPA 5273 (1 alc), Rio Negro (Amazonas Dr.), Novo Air.,o, Arquipélago das Anavilhanas, G.M. dos Santo, 7 Feb 1984; MZUSP 56037 (3 alc), Rio Negro (Amazonas Dr.), 8 km below Tarum.,-mirim (03°07'17"S, 060°08'20"W), J.G. Lundberg, et al., 10 Oct 1994. *Doraops zuloagai*.—**Venezuela**: Zulia: ANSP 179558 (2 skel, 245-256 mm), Rio Catatumbo (Lago Maracaibo Dr.), purchased from fishermen at Encontrados, J.G. Lundberg, et al., 11 Nov 2001, JGL-01-VE1; INHS 54804 (1 alc, 277 mm), Lago Maracaibo (Caribbean Dr.), purchased at Santa Barbara fish market, southern part of lake, J.W. Armbruster, et al., 20 Dec 1999, VEN 99-9. *Doras carinatus*.—**Guyana**: ANSP 177273 (6 alc, 118.0-153.5 mm SL), Essequibo River (Atlantic Dr.), extensive sandbar 2.0 km upstream from Paddle Rock campsite (04°42'20"N, 058°42'26"W), C. Watson, et al., 25 Nov 1997, GGW97-23; ANSP 177275 (1 alc, 188 mm SL), Siparuni River (Essequibo Dr.), blackwater camp and blackwater creek (04°44'21"N, 058°57'54"W), G. Watkins, et al., 4 Dec 1997, GGW97-27; Rupununi: ANSP 180986 (1 skel, 170 mm SL), Essequibo River (Atlantic Dr.) at Yukanopito Falls, 44.5 km SW of mouth of Kuyuwini River (01°54'53"N, 058°31'14"W), M.H. Sabaj, et al., 9 Nov 2003, GUY 03-19. *Doras micropoews*.—"**Guianas**": ANSP 78070 (1 skel, 160 mm SL), Hyrtl Collection; **Guyana**: ANSP 177426 (1 alc, 302 mm SL), Essequibo River (Atlantic Dr.), small blackwater creek opposite Paddle Rock campsite (04°45'00"N, 058°42'00"W), C. Watson, et al., 23 Nov 1997, GGW97-16; ANSP 177880 (5 alc), Essequibo River (Atlantic Dr.), at Essequibo campsite (04°45'41"N, 058°45'53"W), D. Torres, et al., 26 Jan 1997, WGS97-19. *Doras* sp. (Amazonas).—**Brazil**: Amazonas: ANSP 181055 (2 alc), Rio Tefe (Amazonas Dr.), beach at Vista Escura, M. Goulding, 30 Jul 1979; **Colombia**: Vaupés: IAvH-P 2860 (1 alc), Laguna Taraira, Río Apaporis, Apaporis, H. Lopez. *Doras* sp. (Tocantins).—**Brazil**: INPA 18628 (1 alc), Rio Araguaia (Tocantins Dr.), Feb 2000; Goiás: INPA 5244 (1 alc), Rio Araguaia (Tocantins Dr.), Xambioá, Laguinho Central, G.M. dos Santo, 24 Nov 1982; MCP 18188 (2 alc), Rio Araguaia (Tocantins Dr.), lakes near town of Luis Alves (13°14'S, 050°35'W), F.L.T. Garro, Sep 1994. *Doras* sp. (Xingu).—**Brazil**: Mato Grosso: ANSP 181056 [ex MZUSP 87025], (5 alc, 1cs), Rio Curisevo (Xingu Dr.), Porto do Vitorio, prox. ribeirão Kevuaieli, Gaucha do Norte (13°02'05"S, 053°25'19"W), C. Moreira, et al., 19 Oct 2004; Para: ANSP 181057 [ex MZUSP 82297] (1 alc), Rio Xingu (Amazonas Dr.), Belo Monte (03°07'S, 051°42'W), M. Goulding, Jul 1983. *Doras punctatus*.—**Argentina**: Corrientes: ANSP 181012 (1 skel), Rio Parana (left bank) at private park (Club San Martin) near town of Perichon, N of rt. 12, NE of Corrientes, M.H. Sabaj, et al., 11 Apr 2005, ARG 05-04. *Hassar orestis*.—**Venezuela**: Amazonas: ANSP 180294 (4 alc, 1 skel), Rio Ventuari (Orinoco Dr.), beach at village of Moriche, 116 km NE of Macuruco, 169 km NE of San Fernando de Atabapo (04°45'N, 066°21'13"W), M.H. Sabaj, et al., 7 Apr 2004, VEN 04-15; ANSP 180295 (1 skel), Rio Ventuari (Orinoco Dr.), village of Marueta at landing, 91 km ENE of Macuruco, 159 km ENE of San Fernando de Atabapo (04°18'51"N, 066°17'32"W), M.H. Sabaj, et al., 6 Apr 2004, VEN 04-12. *Hemidoras morrissi*.—**Brazil**: Amazonas: ANSP 179174 (3 skel, 118-144 mm SL), Rio Solimoes (Amazonas Dr.) 24.4 km downstream of Sao Antonio do Ica, 12 km upstream of Nova Tonantins (02°54'34"S, 067°50'11"W), J.P. Friel, et al., 24 Nov 1993, JPF-93-136; **Peru**: Loreto: ANSP 180191 (3 alc, 1 skel), Rio Nanay (Amazonas Dr), beach on downstream end of island, just upstream from Santa Clara, W of Iquitos (03°46'45"S, 073°22'06"W), M.H. Sabaj, et al., 14 Aug 2003, PERU 2003-02. *Hemidoras stenopeltis*.—**Brazil**: Amazonas: ANSP 179159 (2 skel, 121-142 mm SL), Rio Amazonas (Atlantic Dr.), 14.4 km downriver of Santa Maria, 35.2 km upriver of Itacoatiara (03°21'22"S, 058°38'52"W), M.W. Westneat, et al., 18 Oct 1994, MWW-94-031; ANSP 179162 (2 skel), Rio Solimoes (Amazonas Dr.) 21.3 km downriver of Tamanicoa, 14.1 km upriver of Palheta (02°35'29"S, 065°29'52"W), J.P. Sullivan, et al., 6 Nov 1993,

- JPS-93-028. *Hypodoras forficulatus*.—**Peru**: Loreto: ANSP 182517 (1 alc), Rio Nanay (Amazonas Dr.), at Pampa Chica, 4.5 km W of Iquitos (03°45'09"S, 073°17'W), M.H. Sabaj, et al., 3 Aug 2005, PERU 05-01; ANSP 182630 (1 skel), Rio Nanay (Amazonas Dr.), large left bank beach upstream from mouth, north of Iquitos (03°42'49"S, 073°16'43"W), M.H. Sabaj, et al., 15 Aug 2005, PERU 05-09. *Leptodoras acipenserinus*.—**Peru**: Loreto: ANSP 182202 (3 alc, 1 skel), Rio Nanay (Amazonas Dr.), upstream half of large beach (left bank) at village of Pampa Chica, 4.5 km W of Iquitos (03°45'09"S, 073°17'00"W), M.H. Sabaj and M.C. Perez, 21 Aug 2005, PERU 05-10. *Leptodoras cataniai*.—**Brazil**: Amazonas: ANSP 179242 (1 skel), Rio Ica (Amazonas Dr.) 2.2 km downstream of Betania and 19.5 km upstream of Sao Antonio do Ica (03°06'24"S, 068°04'09"W), O.T. Oyakawa, et al., 19 Nov 1993, OTO-93-079; Roraima: ANSP 179557 (2 skel), Rio Branco (Negro Dr.) downriver of Atauba and upriver of Caruna (01°20'34"S, 061°52'21"W), J.G. Lundberg, et al., 8 Dec 1993, JGL-93-176; **Peru**: Loreto: ANSP 182201 (7 alc, 1 skel), Rio Nanay (Amazonas Dr.), upstream half of large beach (left bank) at village of Pampa Chica, 4.5 km W of Iquitos (03°45'09"S, 073°17'00"W), M.H. Sabaj and M.C. Pérez, 21 Aug 2005, PERU 05-10. *Leptodoras copei*.—**Venezuela**: Amazonas: ANSP 180298 (2 skel), Rio Ventuari (Orinoco Dr.), village of Marueta at landing, 91 km ENE of Macuruco, 159 km ENE of San Fernando de Atabapo (04°18'51"N, 066°17'32"W), M.H. Sabaj, et al., 6 Apr 2004, VEN 04-12. *Leptodoras hasemani*.—**Guyana**: Rupununi: ANSP 179209 (4 alc, 2 skel), Rupununi River (Essequibo Dr.), at Massara's Landing, 1.1 km NE village of Massara (03°53'41"N, 059°17'37"W), M.H. Sabaj, et al., 26 Oct 2002, GUY 02-05. *Leptodoras juruensis*.—**Brazil**: ANSP 179168 (2 skel, 90-224 mm SL), Rio Amazonas Basin, J.G. Lundberg, et al.; Amazonas: ANSP 179173 (2 skel, 159 mm SL), Rio Solimoes (Amazonas Dr.), 21.3 km downriver of Coadi, 10.2 km upriver of Alvaras (03°09'22"S, 064°49'54"W), O.T. Oyakawa, et al., 30 Oct 1993, OTO-93-006. *Leptodoras linnelli*.—**Venezuela**: Amazonas: ANSP 180296 (5 skel), Rio Ventuari (Orinoco Dr.), village of Marueta at landing, 91 km ENE of Macuruco, 15.9 km ENE of San Fernando de Atabapo (04°18'51"N, 066°17'32"W), M.H. Sabaj, et al., 6 Apr 2004, VEN 04-12. *Leptodoras praelongus*.—**Brazil**: Roraima: ANSP 179156 (3 skel), Rio Branco (Rio Negro drainage) downriver of Atauba and upriver of Caruna (01°20'34"S, 061°52'21"W), J.G. Lundberg, et al., 8 Dec 1993, JGL-93-176. *Lithodoras dorsalis*.—**Brazil**: Para: ANSP 181024 (1 alc, 176 mm), Rio Amazonas (Atlantic Dr.), below mouth of Rio Tapajos, 10.2 km upriver of Monte Alegre (02°05'52"S, 054°00'34"W), L. Rapp Py-Daniel, et al., 4 Nov 1994, LRP-94-010. *Megalodoras guayaensis*.—**Venezuela**: Apure: ANSP 179250 [ex DU F-925] (1 skel), Rio Orinoco basin, probably Rio Apure near San Fernando de Apure, J.G. Lundberg, et al., 1985, JGL-V85-1; ANSP 182983 [DU F-1041] (1 skel, 408 mm), Rio Apure (Orinoco Dr.), J.G. Lundberg, et al., 1985; Delta Amacuro: ANSP 149512 (1 alc), Rio Orinoco, delta at Curiapo, J.N. Baskin, et al., 23 Feb 1978, JNB-77-78; ANSP 177980 (1 alc, 141 mm), Orinoco delta at Los Castillos, J.N. Baskin, et al., 16 Feb 1978, JNB-21-78; ANSP 179167 [ex DU F-1126] (1 skel, 355 mm SL), Rio Orinoco (Atlantic Dr.), downstream from bouy 82, south shore (08°28'24"N, 061°17'12"W), H.L. Lopez, et al., 21 Nov 1979, HLR-40-79. *Megalodoras uranoscopus*.—**Brazil**: Para: ANSP 185328 (1 alc, 195 mm), Rio Amazonas, 26.9 km downstream of Juruti, 46.3 km upstream of Obidos (02°01'40"S, 055°54'37"W), M.W. Westneat, et al., 22 Oct 1994, MWW-94-045; **Peru**: Loreto: ANSP 181184 (5 alc, 1 skel), purchased from ornamental fishermen in Belen, Iquitos, reportedly from Rio Itaya and associated lagoons (Amazon Dr.), M.H. Sabaj, et al., 4 Aug 2005, PERU 05-00B. *Nemadoras elongatus*.—**Brazil**: Amazonas: ANSP 179239 (4 skel), Rio Solimoes (Amazonas Dr.), 24.4 km downstream of Sao Antonia do Ica and 12 km upstream of Nova Tonantins (02°54'34"S, 067°50'11"W), J.P. Friel, et al., 24 Nov 1993, JPF-93-136. *Nemadoras humeralis*.—**Brazil**: ANSP 179161 (2 skel, 83-88 mm SL), Rio Amazonas basin, J.G. Lundberg, et al., 1993; Amazonas: ANSP 179157 (2 skel), Rio Amazonas (Atlantic Dr.), 14.4 km downriver of Santa Maria, 35.2 km upriver of Itacoatiara (03°21'22"S, 058°38'52"W), M.W. Westneat, et al., 18 Oct 1994, MWW-94-031; ANSP 179237 (2 skel, 116-119 mm SL), Rio Amazonas (Atlantic Dr.), below R. Negro, 33.5 km downriver of Manaus, 11.3 km upriver of Jatuarana (03°02'39"S, 059°46'41"W), M.W. Westneat, et al., 12 Oct 1994, MWW-94-013; ANSP 179163 (1 skel, 102 mm SL), Rio Solimoes (Amazonas Dr.) 21.3 km downriver of Tamanicoa, 14.1 km upriver of Palheta (02°35'29"S, 065°29'52"W), J.P. Sullivan, et al., 6 Nov 1993, JPS-93-028; Roraima: ANSP 179238 (1 skel), Rio Branco (Negro Dr.) downriver of Atauba and upriver of Caruna (01°20'34"S, 061°52'21"W), J.G. Lundberg, et al., 8 Dec 1993, JGL-93-176. *Nemadoras leporhinus*.—**Guyana**: Rupununi: ANSP 185097 (10 alc, 1 skel), Takutu River (Branco-Negro Dr.), 3.77 km SSW of Lethem (03°21'18"N, 059°49'51"W), M.H. Sabaj, et al., 1 Nov 2003, GUY 03-03; **Venezuela**: Amazonas: ANSP 180297 (4 alc, 2 skel), Rio Ventuari (Orinoco Dr.), village of Marueta at landing, 91 km ENE of Macuruco, 159 km ENE of San Fernando de Atabapo (04°18'51"N, 066°17'32"W), M.H. Sabaj, et al., 6 Apr 2004, VEN 04-12. *Nemadoras ternetzi*.—**Brazil**: Amazonas: ANSP 179587 (2 skel), Rio Negro (Amazonas Dr.) below R. Branco, 32.4 km downriver of Moura, 9.3 km upriver of Novo Caioe (01°42'04"S, 061°29'01"W), J.N. Baskin, et al., 11 Dec 1993, JNB-93-036; Para: ANSP 179158 (2 skel, 110-122 mm SL), Rio Trombetas (Amazonas Dr.), 5.5 km downriver of Santa Cecilia, 20.9 km upriver of Oriximina (01°37'45"S, 055°58'33"W), F. Langeani, et al., 26 Oct 1994, FL-94-085; **Peru**: Loreto: ANSP 180177 (7 alc, 2 skel), Rio Nanay (Amazonas Dr.), beach on downstream end of island, just upstream from Santa Clara, W of Iquitos (03°46'45"S, 073°22'06"W), M.H. Sabaj, et al., 14 Aug 2003, PERU 2003-02. *Nemadoras trimaculatus*.—**Peru**: Loreto: ANSP 180178 (5 alc, 1 skel) Rio Nanay (Amazonas Dr.), beach on downstream end of island, just upstream from Santa Clara, W of Iquitos (03°46'45"S, 073°22'06"W), M.H. Sabaj, et al., 14 Aug 2003, PERU 2003-02. *Opsodoras morei*.—**Venezuela**: Amazonas: ANSP 183028 (1 skel, 144 mm SL), Rio Negro (Amazonas Dr.), at boat landing in San Carlos de Rio Negro (01°55'15"N, 067°03'48"W), M.H. Sabaj and D.C. Werneke, 19 Mar 2005, VEN 05-34. *Orinocodoras eigenmanni*.—**Venezuela**: Bolivar: ANSP 160255 (1 alc), Rio Guariquito at confluence with Rio Orinoco (07°39'36"N, 66°20'W), B. Chernoff, et al., 25 Nov 1985, V85-56; Delta Amacuro: ANSP 180891 [ex DU F-926] (10 alc, 1 skel), Rio Orinoco on north shore at Isla Portuguesa, ca.

- mi. 117, in Cano Anabata (08°37'20"N, 061°47'30"W), D.J. Stewart, et al., 15 Nov 1979, DJS-14-79. *Oxydoras kneri*.— **Argentina**: Corrientes: ANSP 182203 (1 skel), Rio Parana (Rio de la Plata Dr.), purchased at rivers edge in Esquina, J.G. Lundberg, et al., 13 Apr 2005, ARG 05-06. *Oxydoras niger*.— **Brazil**: Amazonas: ANSP 179160 (1 skel, 178 mm SL), Rio Solimoes (Amazonas Dr.), 21.3 km downriver of Tamanicoa, 14.1 km upriver of Palheta (02°35'29"S, 065°29'52"W), J.P. Sullivan, et al., 6 Nov 1993, JPS-93-028; ANSP 179241 (1 skel), lower Rio Japura (Solimoes Dr.), purchased from fishermen, J.G. Lundberg, et al., 2 Nov 1993; **Peru**: Loreto: ANSP 179438 (1 alc, 3 skel), upper Rio Amazonas basin, purchased live from mercado Belen, Iquitos, M.H. Sabaj, et al., 20 Aug 2003, PERU 2003-00; ANSP 181080 (3 alc, 1 skel), reportedly from Rio Itaya and associated lagoons (Amazon Dr.), purchased from ornamental fishermen in Belen, Iquitos, M.H. Sabaj et al., 4 Aug 2005, PERU 05-00B. *Oxydoras sifontesi*.— **Venezuela**: ANSP 179246 [ex DU F-1092] (1 skel), Rio Orinoco basin, J.G. Lundberg, et al. *Physopyxis lyra*.— **Peru**: Loreto: ANSP 182404 (3 skel), Rio Nanay (Amazonas Dr.), upstream of Iquitos, M.H. Sabaj, et al., 2003. *Platydoras armatulus*.— **Venezuela**: Apure: ANSP 179247 [ex DU F-1105-6] (2 skel, 111-118 mm SL), Rio Claro (Orinoco Dr.), presumably in vicinity of San Fernando de Apure, J.G. Lundberg, et al., 1990. *Platydoras hancocki*.— **Guyana**: Rupununi: ANSP 178748 (1 skel), Rupununi River (Essequibo Dr.), at Massara's Landing, 1.1 km NE of village of Massara (03°53'41"N, 059°17'37"W), M.H. Sabaj, et al., 26 Oct 2002, GUY 02-05; ANSP 180286 (1 alc, 1 skel), Kuyuwini River (Essequibo Dr.), 60.6 km ENE of Kuyuwini Landing, 179 km SE of Lethem (02°11'35"N, 058°42'15"W), M.H. Sabaj, et al., 6 Nov 2003, GUY 03-11; **Venezuela**: Amazonas: ANSP 180989 (1 skel), Rio Ventuari (Orinoco Dr.), at mouth of Cano Camqui, 145 km NNE of Macurucu, 189 km NE of San Fernando de Atabapo (05°03'21"N, 066°19'39"W), M.H. Sabaj, et al., 8 Apr 2004, VEN 04-16. *Pterodoras granulatus*.— **Argentina**: Buenos Aires: ANSP 178799 (3 skel), Rio La Plata (Atlantic Dr.) near La Plata, town of Ensenada fishing pier (34°53'S, 058°09'W), J.G. Lundberg and M. Azpelicueta, 12 Feb 2003, JGL-AR-2003; Corrientes: ANSP 180883 (3 alc, 2 skel), various sites including main and braided side channels and backwaters of R. Parana and lower Guayquiraro, ca. 25 km S of Esquina (30°15'S, 059°36'30"W), J.G. Lundberg, et al., 6 Apr 2005, ARG 05-01; **Brazil**: ANSP 179166 (3 skel, 109-128 mm SL), Rio Solimoes (Amazonas Dr.), J.G. Lundberg, et al., 1993; Amazonas: ANSP 179244 (1 skel), Rio Amazonas (Atlantic Dr.), above mouth of Rio Madeira (03°18'31"S, 058°46'23"W), M.W. Westneat, et al., 13 Oct 1994, MWW-94-026; **Paraguay**: Misiones: UMMZ 207485 (1 alc, 206 mm), Rio Parana, ca. 2 km E of Ayolas (27°24'S, 56°46'12"W), J. Taylor, et al., 25 Aug 1979, P79-95BD. *Pterodoras rivasi*.— **Colombia**: Meta: ANSP 177895 (1 alc, 330 mm), Lake Mozambique (Meta Dr.), Hacienda Mozambique (03°58'N, 073°04'W), J.E. B'hlike, et al., 22 Feb 1972, BFF-7; ANSP 178886 (1 alc, 425 mm), same locality as ANSP 177895, J.E. B'hlike, et al., 24 Mar 1975, BSF-6; **Venezuela**: Apure: ANSP 181068 (7 alc), Rio Apure (Orinoco Dr.), along right bank of channel near Maria Angeles bridge, vicinity of San Fernando de Apure, M.W. Littmann, et al., 9 Apr 2005; Delta Amacuro: ANSP 149539 (1 alc, 157 mm), Rio Orinoco, at upstream mouth of Tres Canos, ca. km. 131.8, J.N. Baskin, et al., 19 Feb 1978; ANSP 177990 (1 alc, 152 mm), Rio Orinoco below Barrancas from buoy at 139 km to 138 km, J.G. Lundberg, et al., 17 Feb 1978, JGL-17-78. *Rhinodoras boehlkei*.— **Ecuador**: FMNH 79203 (1 alc, 136.3 mm, holotype), Rio Bobonaza (Marañon Dr.), between Montalvo and Chicherato, G. Herrera, February 1958; FMNH 88195 (1 alc, 111.8 mm), Rio Bobonaza, (Marañon drainage), G. Herrera, March 1958; **Peru**: Loreto: ANSP 179562 (1 alc, 116.3 mm), INHS 52172 (2, 84.8-118.0 mm), SIUC 39703 (3 alc, 93.3-119 mm), purchased near Iquitos, reportedly from Rio Itaya (Amazonas Dr.), M.H. Sabaj, et al., 28 July 1999. *Rhinodoras dorbigny*.— ANSP 78093 (1 skel, 82.5 mm), Rio de la Plata, Hyrtl Collection; **Brazil**: Rio Grande do Sul: ANSP 179535 [ex MCP 11974] (2 alc), Rio Uruguay, at Rancho da Amizade (28°38'S, 056°02'W), E. Lerner, et al., 12 Dec 1987; ANSP 179536 (1 alc), Rio Uruguay, near Trojan ranch between arroyos Salso and Itapitocai, L. Pena, 6 Oct 1985; **Paraguay**: Presidente Hayes: UMMZ 207627 (1 alc), Riacho Pilco (Pilcomayo drainage) at bridge on dirt road ca. 24.7 km NW of jct. with paved hwy. from Chaco-I to Puerto Falcon (25°06'30"S, 57°46'48"W), J.N. Taylor, et al., 31 Aug 1979, P79-101B. *Rhinodoras thomersoni*.— **Venezuela**: Zulia: INHS 35391 (1 alc), Caño La Yuca at confluence with Rio Escalante (Maracaibo Dr.) (08°49'10"N, 72°00'57"W), L.M. Page, et al., 31 Jan 1995, DCT 95-35; UF 41970 (2 alc, paratypes), Rio Catatumbo (Maracaibo Dr.), at mouth, near El Congo, T. Thorson, et al., 6 Aug 1977. *Rhinodoras* sp. (Branco/Essequibo).— **Guyana**: Rupununi: ANSP 179095 (1 alc, 81.2 mm), Ireng River (Takutu-Branco Dr.), 6.9 km WSW of village of Karasabai (4°01'10"N, 59°36'06"W), M.H. Sabaj, et al., 1 Nov 2002; ANSP 179694 (1 alc, 96.2 mm), Rupununi River (Essequibo Dr.), at Dadanawa cattle ranch (2°49'53"N, 59°31'39"W), M.H. Sabaj, et al., 15 Nov 2003. *Rhinodoras* sp. (Orinoco).— **Venezuela**: Apure: ANSP 165233 (1 alc, 113.1 mm), Rio Apure (Orinoco Dr.), between Rio Portuguesa mouth and San Fernando de Apure airport (7°54'N, 67°32'W), S.A. Schaefer, et al., 4 Nov 1989; MCNG 32703 (1 alc), Rio Apure (Orinoco Dr.), in front of Isla Apurito, O. Castillo and F. Provenzano, 23 Jan 1984. *Rhynchodoras woodsi*.— **Peru**: Loreto: ANSP 181042 (5 alc), Rio Amazonas, vicinity of Iquitos, M.H. Sabaj, et al., 4 Aug 2005, PERU 05-00C. *Trachydoras paraguayensis*.— **Argentina**: Misiones: ANSP 180507 (1 skel), Rio Parana (Rio de la Plata Dr.), eu Nemesio Parma; Corrientes: ANSP 181011 (1 alc, 1 skel), Rio Parana (left bank) at private park (Club San Martin) near town of Perichon, N of rt. 12, NE of Corrientes, M.H. Sabaj, et al., 11 Apr 2005, ARG 05-04. *Trachydoras nattereri*.— **Peru**: Loreto: ANSP 182593 (11 alc, 1 skel), Rio Nanay (Amazonas Dr.), large left bank beach upstream from mouth, N of Iquitos (03°42'49"S, 073°16'43"W), M.H. Sabaj, et al., 15 Aug 2005, PERU 05-09. *Trachydoras steindachneri*.— **Brazil**: Amazonas: ANSP 179171 (2 skel, 89-93 mm SL), Rio Solimoes (Amazonas Dr.) 29.5 km downstream of Sao Antonio do Ica, 5.3 km upstream of Nova Tonantins (02°54'15"S, 067°47'53"W), J.P. Friel, et al., 24 Nov 1994, JPF-93-138.

## Appendix 2

## Comparative pimelodids examined.

*Platysilurus malarma*.—**Venezuela**: Zulia: ANSP 187009 (1 skel, ca. 550 mm SL), market near Encontrados, J.G. Lundberg, et al., 14 Nov 2001. *Platysilurus mucosus*.—**Peru**: Loreto: ANSP 178509 (2 skel), Belem market, Iquitos, M.W. Littmann, et al., 1 Aug 2001. *Pseudoplatystoma tigrinum*.—**Venezuela**: Apure: ANSP 187010 (1 skel, ca. 810 mm SL), Rio Apure at San Fernando de Apure, J.G. Lundberg, et al., 1985.

## Appendix 3

## Key to abbreviations appearing in figures

ANP	anterior nuchal plate (part of nuchal shield)
ANP-MNP-su	anterior-middle nuchal plate suture
bl	Baudelot's (ossified transcapular) ligament
bl-as	Baudelot's (ossified transcapular) ligament attachment site
bl-pv	ventral process (projection) of Baudelot's (ossified transcapular) ligament
BOC	basioccipital
cfo-a	anterior cranial fontanel (anterior to epiphyseal bar)
cfo-p	posterior cranial fontanel (posterior to epiphyseal bar)
CLE	cleithrum
CLE-a	anterior transverse face of cleithrum
CLE-al	anterior lateral face of cleithrum
CLE-COR-b	cleithral-coracoid bridge (under which pass muscles for abducting pectoral spine)
CLE-COR-su	cleithrum-coracoid suture
CLE-ld	dorsal limb of cleithrum
CLE-lh	horizontal transverse (symphyseal) limb of cleithrum
CLE-pad	anterior dorsal process of dorsal limb of cleithrum
CLE-pp	posterior process of cleithrum (= postcleithral or humeral process)
CLE-ppd	posterior dorsal process of dorsal limb of cleithrum
CLE-pp-od	dorsal field ornamentation of posterior process of cleithrum
CLE-pp-om	middle field ornamentation of posterior process of cleithrum
CLE-pp-ov	ventral field ornamentation of posterior process of cleithrum
CLE-pp-rv	narrow ridge along ventral margin of posterior process of cleithrum
CLE-pp-shf	shelf elevating dorsal anterior margin of postcleithral process
CLE-pvp	ventral posterior process of cleithrum (part of cleithral-coracoid bridge)
CLE-shd	shoulder of cleithrum
CLE-shd-shf	shelf on shoulder of cleithrum marking transition to postcleithral process
COR	coracoid
COR-ka	anterior keel of coracoid (on ventral face of horizontal limb)
COR-kp	posterior keel of coracoid
COR-lh	horizontal transverse (symphyseal) limb of coracoid
COR-lv	vertical transverse limb (or wall) of coracoid
COR-pp	posterior process of coracoid
COR-pvl	ventral lateral process of coracoid (part of cleithral-coracoid bridge)
DLS	dorsal-locking spine
EPO	epioccipital
EPO-MNP-su	epioccipital-middle nuchal plate suture
EPO-p	epioccipital process (projects posteriorly)
EXO	exoccipital
FRO	frontal
FRO-SOC-su	frontal-supraoccipital suture
gb	gas bladder

HYO	hyomandibular
hyo-af	articular facet for hyomandibular
INS	infranuchal scute
INS-wd	dorsal wing of infranuchal scute
INS-wv	ventral wing of infranuchal scute
is	interorbital septum (composed of parasphenoid and adpressed orbitosphenoids)
LAC	lacrimal
LET	lateral ethmoid
MET	mesethmoid
MNP	middle nuchal plate (part of nuchal shield)
MNP-wa	anterior wing of middle nuchal plate
orb	bony orbital rim dorsally enclosing eye
ORS	orbitosphenoid
PAS	parasphenoid
PCS	pectoral-fin spine
PCS-da	anterior dentations of pectoral-fin spine
PCS-dp	posterior dentations of pectoral-fin spine
PCS-pa	anterior process of pectoral-fin spine
PCS-pv	ventral process of pectoral-fin spine
PNP	posterior nuchal plate (part of nuchal shield)
PNP-wp	posterior wing of posterior nuchal plate
PNP-wv	ventral wing of posterior nuchal plate
PRO	prootic
PTO	pterotic
PTO-EPO-su	pterotic-epioccipital suture
PTS	pterosphenoid
PTT-SCL	posttemporal-supracleithrum
PVO	prevomer (= vomer)
RB1	1st complete rib (borne on 6th vertebra)
SOC	supraoccipital
SOC-ANP-su	supraoccipital-anterior nuchal plate suture
SOC-k	keel of supraoccipital process
SOC-mp	middle pitline (transverse groove) of supraoccipital
SOC-n	notch in supraoccipital process
SOC-p	supraoccipital process
SOC-r	paired ridges of supraoccipital process
SOC-t	trench in supraoccipital process
SPO	sphenotic
SPO-s	sphenotic spine
SPO-ts	sphenotic transverse strut
ta	tympanic area
TS3	third tympanal scute
VC	vertebral centrum (first = VC1, second = VC2, etc.)
VC4-mr	Müllerian ramus (= anterior limb of parapophysis) of 4th vertebra
wc	Weberian complex

---

## Appendix 3

Measurements (in mm) of postcleithral process and pectoral spine of fossil and modern *Doraops zuloagai*

	ANSP 179558 (skel)		ANSP 179558 (skel)		INHS 54804 (alc)		UNEFM-PF-0278 (fossil)	
Total length	295		305		340		831–941* 890–927**	
Standard Length	245		256		277		690–767* 725–770**	
Postcleithral process	left	right	left	right	left	right	left	
Ventral length	31.2	29.8	30.2	30.4	33.5	31.8	48.2	
Depth	6.5	6	6.6	7	7.9	7.8	18.5	
Ventral length/depth	4.8	5.0	4.6	4.3	4.2	4.1	2.6	
Pectoral spine	left	right	left	right	left	right	left	
Width	5.4	5.5	5.4	5.4	5.6	5.7	15.5	
Depth	3.5	3.6	3.7	3.7	4.2	4.2	11	
Width/depth	1.5	1.5	1.5	1.5	1.3	1.4	1.4	

\* Based on width of pectoral spine in modern specimens.

\*\* Based on depth of pectoral spine in modern specimens.

## Appendix 4

Measurements (in mm) of skull of fossil *Platysilurus* sp.

Measurement	UNEFM-PF 0412	UNEFM-CIAAP 1359
Maximum midline length, dorsal	260	253
Maximum midline length, ventral	210	—
Maximum width across sphenotics	174	158
Maximum length of supraoccipital process	62	59
Maximum width of supraoccipital process	—	42
Maximum width at anterior end of hyomandibular facet	138	125
Maximum width at posterior end of hyomandibular facet	102	130
Hyomandibular facet length	51	60
Basioccipital condyle width	47	—
Basioccipital condyle height	50	—